An original approach combining biogeochemical signatures and a mixing model to discriminate spatial runoff-generating sources in a peri-urban catchment

Olivier Grandjouan[1#], Flora Branger[1], Matthieu Masson[1], Benoit Cournoyer[2], Nicolas Robinet[3], Pauline Dusseux[4], Angélique Dominguez Lage[2], Marina Coquery[1]

[1] INRAE, UR Riverly, 5 rue de la Doua, F-69625, Villeurbanne, France
[2] Univ Lyon, UMR Ecologie Microbienne (LEM), Université Claude Bernard Lyon 1, VetAgro Sup, France
[3] UMR CNRS 5194 Pacte, Université Grenoble Alpes, Cermosem, 1064 chemin du Pradel, 07170 Mirabel, France
[4] Institut d'Urbanisation et de Géographie Alpine, Université Grenoble-Alpes, CNRS, PACTE, 38100, Grenoble, France

Correspondence to: Olivier Grandjouan (olivier.grandjouan@insa-lyon.fr)

#: present address: INSA Lyon, DEEP, UR7429, 69621 Villeurbanne, France

Abstract.

Hydrograph separation using biogeochemical data is a commonly used method for the vertical decomposition of flow into surface, subsurface and groundwater contributions. However, its application to the spatial decomposition of flow remains limited, despite its potential to identify contributions linked to geological, pedological, and land use characteristics, as well as anthropogenic contaminant sources. In this study, a Bayesian mixing model was applied to the Ratier peri-urban sub-catchment of the OTHU Yzeron observatory. Eight runoff-generating sources were identified and sampled, including different land uses (e.g. forest, grassland, agricultural areas), a colluvium aquifer, and urban point discharges (e.g. sewer system, urban and road surface runoff). A wide range of biogeochemical parameters were analysed including classical (i.e., major chemical compounds, dissolved metals) and innovative tracers (i.e., characteristics of dissolved organic matter, microbial indicators). Streamwater samples collected under contrasting hydro-meteorological conditions revealed distinct source signatures and highly variable contributions, with wastewater dominating under dry weather and rapid surface runoff during summer storms. Using these results, we improved a previously designed perceptual hydrological model of the Ratier and Mercier catchments, at the hillslope scale, which highlighted the potential of spatial tracer-based decomposition in addition to classical vertical hydrological separation. More broadly, this study demonstrates the potential of such mixing model, using classical but also more innovative tracers, to provide insights for validating distributed hydrological models and to anticipate the influence of land use, urbanisation, and climate changes on runoff generation.

Keywords: runoff-generating sources, fingerprints, spatial decomposition, geochemical tracers, Yzeron

1. Introduction

Peri-urban catchments are characterised by contrasting landscapes that can include natural areas (e.g. forests, moorlands), agricultural areas (e.g. crops, grassland) and urban areas (e.g. residential, commercial or industrial areas). These catchments are under considerable pressure from increasing urbanisation, particularly around large cities (Mejía and Moglen, 2010). Peri-urban landscapes are evolving quickly as natural and agricultural areas are decreasing in favour of urban areas (Jacqueminet et al., 2013). This increasing urbanisation can alter water pathways and increase transfer of anthropogenic contaminants, leading to serious deterioration of surface water and groundwater quality.

Sewer overflows are major vectors for a large number of contaminants such as organic matter, organic micropollutants, trace metal elements (e.g. Cu, Ni, Pb, Zn), nutrients or pathogens (Chocat et al., 2001; Lafont et al., 2006; Pozzi et al., 2024; Walsh et al., 2005). Impervious surfaces act as vectors for many contaminants, via rainwater runoff on urban surfaces, such as certain metals (e.g. Cu, Pb, Zn; Charters et al., 2016) or polycyclic aromatic hydrocarbons (Bomboï and Hernandez, 1991), and microbes (Bouchali et al., 2024). Agricultural activities can also bring significant contributions of contaminants in water such as pesticides (Giri and Qiu, 2016), veterinary products (Martins et al., 2019), animal faecal contamination (Marti et al., 2017) or nutrients via fertilization (Penuelas et al., 2023). Small catchments (~10 km²) are particularly sensitive to the degradation of the surface water quality, as they generally consist of streams close to contaminant sources associated with low dilution capacity (Giri and Qiu, 2016). Effective management of water resources and water quality requires precise knowledge of the water pathways and sources in peri-urban catchments (Gonzales et al., 2009). However, identifying runoff-generating sources and estimating their contribution is difficult, as direct measurement of each contribution is almost impossible (Tardy et al., 2004).

Runoff-generating sources are numerous in peri-urban catchments and can be of different kinds due to the diversity of land uses and the presence of artificial elements that divert water such as sewer systems, sewer overflow devices and impervious areas (Birkinshaw et al., 2021; Jankowfsky, 2011). These sources can be defined as hydrological components (e.g. surface runoff, soil water or groundwater flow; Cooper et al., 2000), as specific land uses (e.g. forest, agriculture, urbanized area; Ramon, 2021), or as point contribution (e.g. sewer overflow or wastewater treatment plant outlet; Pozzi et al., 2024). Runoff-generating sources can also be considered as sub-catchments representing a combination of specific geological, pedological and land use factors (Barthold et al., 2010).

It is now recognised that the biogeochemical composition of water can provide information on the contributions of runoff-generating sources, which cannot be deduced from rainfall-runoff dynamics alone (Birkel and Soulsby, 2015). The use of geochemical signatures through a mixing model is now commonly applied to estimate contributions of runoff-generating sources to streamflow (e.g. Burns et al., 2001; Christophersen et al., 1990; Ladouche et al., 2001; Lamprea & Ruban, 2011; McElmurry et al., 2014). To this day, this approach has been applied to estimate contributions from a wide variety of sources such as groundwater flow, subsurface flow and surface runoff (Gonzales et al., 2009; Ladouche et al., 2001), snow and glacier melt (Kumar et al., 2024; Rai et al., 2019; Wellington and Driscoll, 2004), sources of nutrients (Kaown et al., 2023; Verseveld

et al., 2008; Wang et al., 2024), sources of sediments (James et al., 2023; Klages and Hsieh, 1975; Vale et al., 2022), or to study the impact of different forest management methods on water quality (Fines et al., 2023; Motha et al., 2003). However, this approach has rarely been applied to estimate contributions from both vertical and spatial runoff-generating sources, although it shows strong potential for spatial decomposition according to sources linked to the geological, pedological and land use characteristics of the catchment (Nascimento et al., 2023; Liu et al., 2023; Uber et al., 2019). In addition, the use of tracers is often limited to classical geochemical tracers such as stable isotopes, major ions (Singh and Stenger, 2018) or metals (Barthold et al., 2010). Yet, many other biogeochemical parameters show potential for discriminating additional sources, such as the characteristics of dissolved organic matter (Begum et al., 2023; McElmurry et al., 2014; Sun et al., 2024) or microbial parameters (Colin et al., 2020; Marti et al., 2017).

The objective of the present study is to identify runoff-generating sources linked to both vertical and spatial characteristics of a small peri-urban catchment (e.g. geology, land use), and estimate their contributions to streamwater in contrasted hydro-meteorological conditions. This approach is based on the creation of a large biogeochemical dataset through the sampling and analysis of runoff water in a catchment. Classical and innovative tracers were used as input data in a mixing model. We applied this approach to the Ratier peri-urban catchment, and its nested Mercier sub-catchment, in France, to better understand their hydrological behaviour and to identify potential sources of contamination. First, we present the sampling campaigns for runoff-generating sources and streamwater, as well as sample pre-treatment and analysis. Then, we describe the characterization of biogeochemical signatures of the sources and their contributions to streamwater obtained via hydrograph separation. Finally, we discuss the estimated signatures and contributions for each source, then propose a revision of the initial perceptual hydrological model presented by Grandjouan et al. (2023), to provide a better understanding of the Ratier and Mercier catchments hydrological behaviour.

2. Materials and methods

2.1 Study area: the Ratier catchment

The Ratier catchment is located west of Lyon, in France. It is part of the Yzeron basin and a site of the Field Observatory in Urban Hydrology (OTHU; https://www.graie.org/othu/) and the Critical Zone Observatories: Research and Application OZCAR (https://www.ozcar-ri.org/). It covers an area of 19.8 km² and has an altitude ranging between 250 and 780 m. The catchment climate is temperate with Mediterranean and continental influences (Gnouma, 2006). The bedrock is predominantly crystalline with gneiss underlying 96% of the total surface (Figure 1.A). The shallower part of the gneiss is fractured and provides low perennial groundwater storage (Delfour et al., 1989) The fractured gneiss gradually changes to a weathered clayous-sandy saprolite layer, which varies from less than 1 m thick in the upper part of the catchment to 10 to 20 m in the valley bottom (Goutaland, 2009). The delimitation between this layer and the thin sandy to loamy soils is not clear (Braud et al., 2011). The soils are associated with low to medium field capacities, with the exception of valley bottoms characterised by high field capacities (Figure 1.B). Downstream of the catchment, the eastern part is covered by colluvium deposits holding a

local aquifer (Figure 1.A). This catchment is typically peri-urban with 48% of agricultural areas, 30% of forest and 21% of urban areas (Jacqueminet et al., 2013). Field surveys performed by Bétemps (2021) provided information about agricultural activities, which include cereal crop cultures (10% of the catchment area), bovine (10%) and equine breeding (2%) (Figure 1.C). In the urbanized areas, wastewater and rainwater are managed by a combined sewer network and transferred outside the limits of the catchment; however, they can be released in streams during rainstorms via a sewer overflow device located directly upstream of the Ratier outlet (Figure 1.D). The Mercier stream is a tributary of the Ratier stream with a catchment area of 7.8 km². Its geology consists entirely of gneiss bedrock. Land use is predominantly agriculture (49%) and forest (38%), with a small proportion of urban areas (13%), including therefore less rainwater drainage facilities than the Ratier catchment. The Pollionnay, Col de la Croix du Ban and Col de la Luère pluviometric stations (Fig. 1.D) records rain and air temperature since 1997, 2005 and 2009, respectively. The mean annual precipitation is 750 mm and the mean annual minimum and maximum temperatures are 6.6 and 18.4°C from 2010 to 2022 (Grandjouan, 2024). Two gauging stations located at the outlets of the Mercier and Ratier catchments allow a continuous hydrological monitoring since 2010 and 1997, respectively (Figure 1.D). Hydrological data show a contrasted hydrological regime, with marked low-flow periods between June and September, particularly upstream where runoff is low throughout the year. The Mercier stream is frequently observed to be dry, unlike the Ratier stream, which is continuously supplied by the colluvium aquifer (Grandjouan et al., 2023). According to the rain and discharge data, the response time (i.e., the time elapsed between the peak of rainfall and the corresponding peak in discharge) for the Ratier catchment is around 30 minutes.

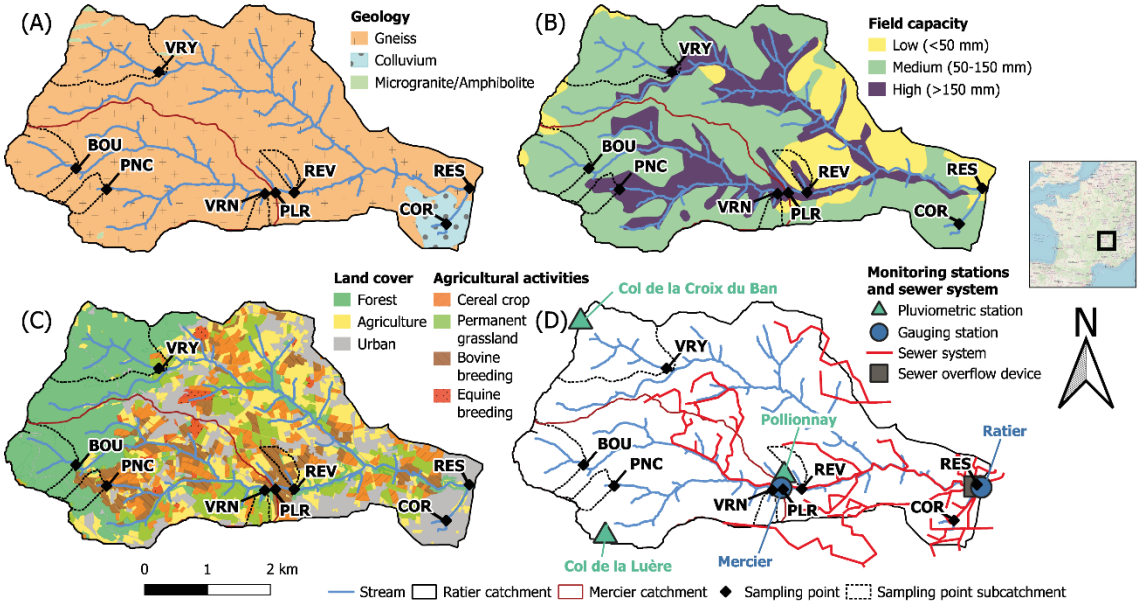

Figure 1 – Maps of the Ratier and Mercier catchments showing the sampling points (see Table 1 for details) and (A) geology (David et al., 1979; Delfour et al., 1989; Gnouma, 2006), (B) field capacity (Labbas, 2014), (C) land use (Jacqueminet et al., 2013) and agricultural activities (Bétemps, 2021) and (D) monitoring stations and sewer system (from Grand Lyon and SIAHVY).

2.2 Field data acquisition

2.2.1 Source identification and sampling

In this study, we mainly considered runoff-generating sources as homogeneous sub-catchments associated with a combination of representative factors including geology, field capacity, land use and agricultural activities. We based our work on the hypothesis that the biogeochemical composition of streamwater at the outlet of each sub-catchment is representative of its associated factors (Barthold et al., 2010).

The first step in identifying these sources involved the superposition of geological, field capacity, land use and agricultural activities maps (Figure 1). In this way, we identified the most spatially representative combinations of factors in the catchment, as detailed in Table A1. Based on these results, we identified the main sources and named them according to their associated land use: forest (FOR), grassland (GRA), agriculture (AGR), colluvium aquifer (AQU), and urban and road surface runoff from impervious areas (URB) (see Table 1). We considered quick surface runoff from other areas (SUR) as an additional source, resulting from infiltration excess or saturation excess overland flow (Beven, 2012). We identified wastewater (SEW) as a last source that can be discharged from the combined sewer system into the stream via an overflow device located downstream of the Ratier catchment (Figure 1.D), or other overflow pipes.

Then, we selected sampling points representative of each source. These points are located at the outlet of selected sub-catchments (Table 1 and Figure 1), according to the predominant combination of factors as well as field surveys, which allowed to check the consistency of land use, particularly for agricultural activities that may evolve from year to year. The presence of a permanent flow, even a weak one, at the sub-catchment outlets was also a requirement for the sampling points selection. We selected the colluvium groundwater sampling point (COR) in the upstream section of a stream draining this aquifer. In the case of FOR and GRA sources, we selected two sampling points for each source to compare the biogeochemical signatures obtained from two sub-catchments of the same type (i.e., BOU and VRY, VRN and REV, respectively). The agricultural sub-catchment (PNC) includes bovine breeding and cereal crops. For the URB runoff, we selected a storm water discharge point (PLR) fed by runoff from a road and an upstream urban area. For the SUR runoff, we planned to collect direct surface runoff during rainfall events, directly from the surface of forest and agricultural sub-catchments (BOU, VRY, REV and PNC). In order to approach sewer system overflow condition, we collected wastewater directly in the sewer system (RES) during rainy period.

Table 1 – Identified runoff-generating sources and corresponding sampling points with their relative sub-catchments areas, geology, field capacity, land use and main features, based on information provided in Figure 1 and field observations. n.a. : non available

Source		Sampling point	Sub-catchment area (ha)	Geology	Field capacity[1]	Land use (%) and main features					
Code	Description					Forest		Agriculture		Urban	
AQU	Colluvium aquifer	COR	-	-	-	-		-		-	
FOR	Gneiss / Medium field capacity / Forest	BOU	88	Gneiss	Medium	Deciduous, coniferous	100	-	0	-	0
		VRY	151	Gneiss	Medium	Deciduous, coniferous	100	-	0	-	0
GRA	Gneiss / Medium to high field capacity / Grassland	VRN	13	Gneiss	Medium	Decidous	30	Grassland	70	-	0
		REV	18	Gneiss	Low to high	Decidous	30	Grassland	70	-	0
AGR	Gneiss / Medium field capacity / Agriculture	PNC	22	Gneiss	Medium to high	-	40	Grassland, bovine breeding, cereal crop	25	Landfill	15
URB	Urban and road surface runoff	PLR	-	-	-	-	-	-	-	-	-
SUR	Quick surface runoff	n.a.	-	-	-		-		-		-
SEW	Sewer system	RES	-	-	-	-	-	-	-	-	-

[1] Among low, medium and high field capacities identified by Labbas (2014).

In order to assess the seasonal variability of the biogeochemical water composition, we sampled sources in contrasted hydro-meteorological conditions. We considered low flow conditions from June to September, and high flow conditions from October to May. We considered wet weather conditions when the cumulative rain over 5 days exceeded 3 mm, and dry weather when it was below 3 mm, this value being the median of daily rainfall recorded between 2011 and 2023 at the Pollionnay station. We performed eight source sampling campaigns between February 2022 and March 2023. We collected 4 to 5 water samples manually for each sampling point, for a total of 38 source samples.

Some field observations differed from the initial information provided in Figure 1: no bovine breeding was observed at REV during the campaigns, whereas cereal crops were observed at PNC; no direct surface runoff was observed during the campaigns at BOU, VRY, VRN and REV, so we could not sample the SUR source.

2.2.2 Streamwater sampling during hydrological events

We also sampled streamwater at the outlet of the Mercier and Ratier catchments, targeting contrasted hydrological events. To do so, we extracted past hydrological events from the data available for years 2011-2021, and analysed them following the approach presented by Braud et al. (2018). We calculated seven hydro-meteorological indicators to characterise the 315 extracted events, namely, duration of rain, cumulative rainfall, total runoff, 5-day cumulative reference evapotranspiration, dry

period duration, antecedent precipitation index, and 5-day cumulative rainfall (Figure 2). Based on a Hierarchical Clustering Analysis (HCA), the events were classified according to these indicators. We identified an optimal number of three classes using the "elbow" method (Thorndike, 1953); then, assigned a class to the different types of events: small winter events, summer storm events and major events. Figure 2 shows a Principal Component Analysis (PCA) visualisation of this classification. Major events are defined by high precipitation rate, long duration and high total runoff volume. Summer storm events are characterised by a long dry period before the beginning of the event and high evapotranspiration rate. Small winter events represent the majority of the extracted events and are characterised by low values for all the indicators. Antecedent precipitation index (API), which corresponds to the sum of daily precipitation weighted according to a multiplying factor (k = 0.8; Sarrazin, 2012), and the cumulative rainfall 5 days (R5) before the event, did not mark any specific event class. Based on this classification, we defined a sampling objective of two hydrological events by class to study intra-class variability and taking in account the difficulty of targeting major and summer storm events.

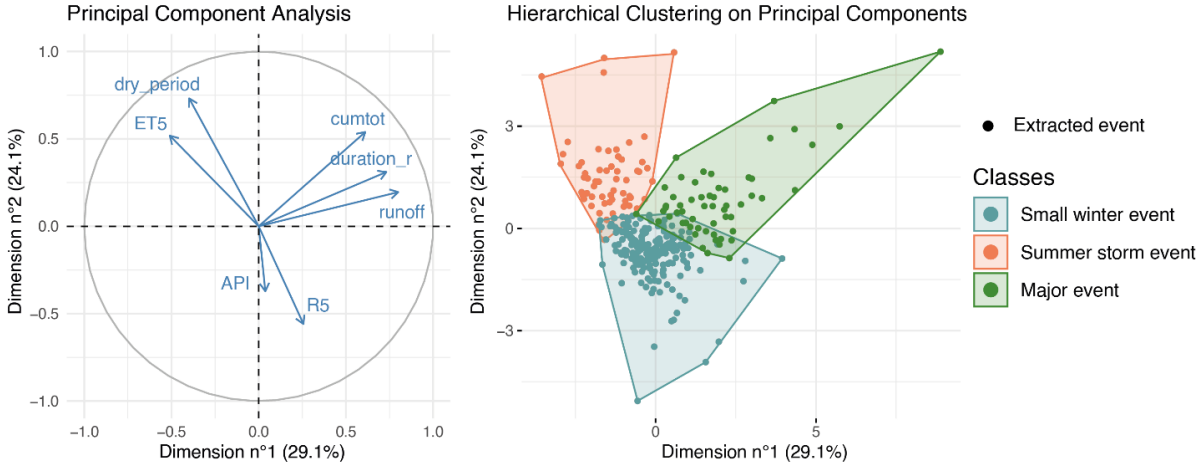

Figure 2 – Principal Component Analysis visualisation of the hydrological event classification based on a Hierarchical Clustering Analysis. duration_r: duration of raining event; cumtot: cumulative rain during the event; runoff: total runoff during the event; ET5: cumulative reference evapotranspiration 5 days before the event; dry_period: duration of dry period before the event; API: antecedent precipitation index at the beginning of the event; R5: cumulative rain 5 days before the event.

We used automatic samplers (Endress+Hauser Liquiport CSP44) to sample streamwater at the Mercier and Ratier gauging stations (Figure 1). We carried out a weather alert to launch the sampling campaigns according to the targeted hydrological events. We adapted sampling time steps to each event, from 10 to 45 minutes, according to the expected duration of the rain. Six hydrological events were sampled between March 2019 and March 2023, ensuring two events per class. The March 2019 and June 2022 events were not sampled at the Ratier and Mercier station, respectively, due to technical issues on the automatic samplers. We obtained 20 to 24 samples for each event, and mixed them two by two in order to ensure sufficient volume for

analysis. After pairing, 10 to 12 samples were finally obtained for each event and at each gauging station. Table 2 shows the hydro-meteorological indicators calculated for these events.

Table 2 – Hydro-meteorological indicators calculated for the hydrological events sampled at the Mercier and Ratier gauging stations. The Sampled station column indicates at which gauging station the event was sampled. duration_r: duration of raining event; cumtot: cumulative rain during the event; runoff: total runoff during the event; ET5: cumulative reference evapotranspiration 5 days before the event; dry_period: duration of dry period before the event; API: antecedent precipitation index at the beginning of the event; R5: cumulative rain 5 days before the event.

Event sampling campaign	duration_r (h)	cumtot (mm)	runoff (mm)	ET5 (mm)	dry_period (h)	API (mm)	R5 (mm)	Event class	Sampled station
06/03/2019	20	7	0.3	8	55	0	3	Small winter event	Mercier
10/05/2021	44	92	11.6	13	70	0	10	Major event	Mercier/Ratier
03/10/2021	80	89	5.8	13	147	0	0	Major event	Mercier/Ratier
22/06/2022	116	57	0.3	38	291	0	0	Summer storm event	Ratier
14/09/2022	44	9	0.1	15	94	0	2	Summer storm event	Mercier/Ratier
13/03/2023	19	18	0.7	7	13	1	27	Small winter event	Mercier/Ratier

2.2.3 Streamwater sampling during dry weather

We also considered streamwater composition at dry weather. Data used come from an available dataset described in Grandjouan et al. (2023). In this study, monthly monitoring campaigns were conducted from March 2017 to December 2019 at the outlets of the Mercier and Ratier catchments; a total of 24 samples were collected manually. These samples were classified into low flow (June to September) and high flow (October to May) conditions.

2.2.4 Sample pre-treatment and analysis of biogeochemical parameters

All source and streamwater samples were filtered at 0.45 µm and analysed for a set of 35 biogeochemical parameters in order to obtain a more accurate characterisation and discrimination of the identified sources. This list includes geochemical parameters, characteristics of the dissolved organic matter (DOM), and two microbial parameters (Table 3). Classical tracers like major ions, silica and trace elements were selected as they can be closely related to geological characteristics of the catchments, particularly Ca^{2+}, SiO_2 and Sr for crystalline formations like gneiss (Fröhlich et al., 2008b; White et al., 1999). They can also be helpful to trace the contribution of agricultural activities as K^+ (Cooper et al., 2000), Cd (El Azzi et al., 2016), Cu (Vian, 2019) or As (Yokel and Delistraty, 2003). Trace metals can trace urban origin of water, as for Cd, Cr, Cu, Ni, Pb, Rb or Zn (Becouze-Lareure, 2010; Coquery et al., 2011; Froger et al., 2020; Lamprea and Ruban, 2011). Finally, major ions such as K^+ and Na^+ can be observed at high concentrations in wastewater (Fröhlich et al., 2008). We selected UV-Visible and HPSEC indicators as they can represent both natural and anthropogenic sources by characterising the molecular weight of DOM. The spectral slope S1 is inversely correlated with this molecular weight and high S2 values are more likely to be associated with terrestrial MOD, compared to fresh algal MOD (Helms et al., 2008). The HPSEC indicators A0, A1, A2 and

A3 represent very large, large, small and very small molecules, respectively (Boukra et al., 2023). We selected the *HF183* and *rum-2-bac* host-specific microbial DNA targets to detect and trace faecal contamination from human and ruminant, respectively.

Additional parameters were analysed for these samples but not used in the present study. The full set of 55 biogeochemical parameters is available at : https://entrepot.recherche.data.gouv.fr/dataverse/chypster/ (Masson et al., 2025a, b).

Geochemical parameters included 6 major ions, silica and 15 trace metal elements. Major ions were analysed by ion chromatography, silica by colorimetry and trace elements by inductively coupled mass spectrometry (ICP-TQ-MS). The absence of contamination was systematically verified by the analysis of blanks. Limits of quantification (LQ) and analytical uncertainties are detailed in Table A2. The accuracy and uncertainties of the methods were routinely checked using certified standard solutions and reference materials, as well as regular participation in interlaboratory testing.

Characteristics of the DOM included Dissolved Organic Carbon (DOC) concentrations, two Ultra Violet-Visible (UV-Vis) indicators and five High Pressure Size Exclusion Chromatography (HPSEC) indicators. The DOC analyses were performed by high temperature catalytic combustion. The UV-Vis indicators were calculated from absorbance spectra obtained between 200 and 800 nm from UV-Visible spectrophotometry analyses, as described by Li & Hur (2017) and Boukra et al. (2023). The HPSEC analyses were performed as described by Boukra et al. (2023) and HPSEC indicators were calculated from chromatogram obtained with UV detection at a wavelength of 254 nm according to Peuravuori & Pihlaja (1997).

Microbial parameters included two host-specific microbial DNA targets, markers of human faecal bacterial contamination (*HF183* DNA target) and ruminant contamination (*rum-2-bac* DNA target). Targets were tracked using a quantitative Polymerase Chain Reaction method (qPCR). The DNA extractions were performed as indicated in Pozzi et al. (2024) and the qPCR assays performed according to Bouchali et al. (2024).

Table 3 – Measured biogeochemical parameters and analytical methods. The tracers in bold correspond to the final selection of tracers used in the mixing model (see Section 3.2).

Parameter family	Biogeochemical parameter	Analytical method
Major anions	**Cl^-**, **SO_4^{2-}**	Ionic chromatography NF EN ISO 14911 (1999)
Major cations	**Ca^{2+}**, **K^+**, **Mg^{2+}**, **Na^+**	Ionic chromatography NF EN ISO 10304-1 (2009)
Silica	**SiO_2**	Colorimetry NF T 90-007 (2001)
Dissolved metals	Al, **As**, B, **Ba**, Cd, Co, **Cr**, Cu, **Li**, Mo, Ni, Pb, **Rb**, **Sr**, Ti, U, V, Zn	ICP-MS NF T 90-007 (2001)
Dissolved organic carbon	**DOC**	Dosage NF EN 1484
UV-Visible indicators	S1, **S2**	UV–visible spectroscopy
HPSEC indicators	Mn-254, A0-254, A1-254, A2-254, A3-254	High Pressure Size Exclusion Chromatography
Microbial qPCR assays	*Human marker Bacteroides (HF183)*, *ruminant marker Bacteroides (rum-2-bac)*	qPCR

2.2.5 Quick surface runoff from non-urban areas

As no surface runoff could be sampled for the SUR source, we considered that the biogeochemical composition of quick surface runoff away from impervious areas was close to the composition of rainwater, assuming that it does not have enough time to acquire significant biogeochemical elements from the soil it flows over. Such hypothesis is supported by the concentrations of several parameters in streamwater during rainy weather (e.g. Cl^-, SO_4^{2-}, SiO_2, Mg^{2+}, Na^+), which are lower than all concentrations measured in the source samples. This observation suggests dilution by low-mineralised inputs. However, this assumption does not take into account the enrichment of water by soil leaching. Therefore, we examined final results considering that this assumption may lead to an underestimation of the quick surface runoff contribution when applying the mixing model for hydrological events (see Sections 4.1 et 4.2). The SUR source was associated to rainwater composition obtained at the Pollionnay pluviometric station (Figure 1; Lagouy et al., 2022), sampled between 2017 and 2023, for major ions, DOC and UV-Vis indicators ($n = 9$). We used data from the Ecully pluviometric station (10 km from Pollionnay) for trace metal element concentrations, produced by (Becouze-Lareure, 2010) between 2008 and 2009 ($n = 32$). No data was available for HPSEC and microbial indicators for the quick surface runoff source.

2.3 Characterization and biogeochemical signatures of runoff-generating sources

2.3.1 Biogeochemical composition and typology of runoff-generating sources

All data obtained from the 38 source water samples and the 35 analysed parameters were used to provide a global characterization of the biogeochemical composition for each source. This description was used to compare the biogeochemical composition of the identified sources, as well as to study their variability according to the hydro-meteorological conditions, in order to confirm similarities, and thus the grouping of samples collected from the same type of source (BOU and VRY for forest; VRN and REV for grasslands) or, on the contrary, the distinction between groups of samples. We used a Hierarchical Clustering Analysis (HCA) to classify the samples according to the biogeochemical dataset and to create a typology of sources. We applied HCA based on an optimal number of class determined with the "elbow" method (Thorndike, 1953), using absolute concentrations that we centred and scaled. The purpose of this typology is to describe the nature of the sources that will be considered in the mixing model.

2.3.2 Building-up the biogeochemical signatures

A biogeochemical signature can be defined as a limited selection of discriminating and representative tracers. Using selected tracers, we built biogeochemical signatures that fed a mixing model to estimate the contribution of sources at the catchment outlet. The tracers must be additive, discriminating, and must be considered as conservative through the mixing process (Christophersen and Hooper, 1992; Stock et al., 2018; Tiecher et al., 2015) (see section 2.4 for more details on the assumptions required when applying a mixing model). We applied a reductionist tracers selection approach based on the biogeochemical dataset for 35 parameters. This approach aimed at selecting the smallest combination of tracers showing the highest inter-source variability and the lowest intra-source variability.

All major parameters and metals were considered additives regarding their chemical characteristics (Benjamin, 2014). The bacterial DNA targets *HF183* and *rum-2-bac* bacterial DNA targets show undefined relations with abiotic parameters, which prevent their use in a mixing model. Although we discarded them from the reductionist tracer approach, we used them afterwards to evaluate the biogeochemical signatures and the estimations obtained.

We eliminated non-conservative parameters by applying a range-test method (Sanisaca et al., 2017; Wilkinson et al., 2013), that check that the concentrations measured in a mixture (here the streamwater sampled at the Mercier and Ratier outlets during the hydrological events) are comprised within the limits represented by the concentrations observed in the source samples. Failure of this test suggested a non-conservative parameter or a missing source (Collins et al., 2017). We then eliminated non-discriminating parameters using a Kruskal-Wallis test (Kruskal and Wallis, 1952) followed by a Dunn post hoc test (Dunn, 1964), with a p-value threshold of 0.05. The null hypothesis is that the distributions of each parameter are identical across all groups; parameter for which this hypothesis could not be rejected are considered non-discriminating. Lastly, we selected the most discriminating tracers using a Linear Discriminant Analysis (LDA) coupled to a Wilks lambda approach (Collins et al.,

1997). We used the remaining tracers to build the biogeochemical signatures of the runoff-generating sources, in the form of radar plots, using min-max standardized concentrations to obtain values between 0 and 1.

2.4 Estimation of the source contributions at the outlet of the catchments

We applied a mixing model to decompose streamwater for samples collected at the Ratier and Mercier sub-catchment outlet stations. We respected the basic assumptions when applying a mixing model provided by Stock et al. (2018), suggesting that a user must verify that : (1) all sources which contributes to streamwater are identified, (2) the signature from source to the mixture is not altered (see Section 2.3.2), (3) the source signatures are fixed, (4) the contributions sum to 100% and the signature of sources differ. We estimated the source contributions during dry weather and during the six targeted hydrological events. In the absence of rain, we did not consider urban/road surface runoff and quick surface runoff as sources contributing to the streamwater samples. We chose a Bayesian approach to resolve the mixing model equations, using the package *MixSIAR* in R (Stock et al., 2018). This approach allows for the incorporation of uncertainty in both source and mixture data, and provides an estimate of the uncertainty associated with the model-derived source contributions, as quantified by the posterior distributions. Hereafter, the term "uncertainty" refers to this model-derived uncertainty. The prior information chosen for source contributions, representing the initial assumption about the relative contributions of each source, correspond to *1/n*, where *n* is the number of sources considered. The prior information on the biogeochemical parameter concentration for the sources, representing the initial assumption about these concentrations, was modelled as a normal distribution, defined by the mean and covariance matrix of the measured concentration.

3. Results

3.1 Biogeochemical composition and typology of runoff-generating sources

The median and range of concentrations of the biogeochemical parameters measured at the sampling points are reported in Table A3 for major parameters, Table A4 for metals, Table A5 for the characteristics of DOM and Table A6 for the microbial parameters. Concentrations are illustrated in the form of a heatmap in Figure 3, coupled with a Hierarchical Cluster Analysis on the parameters and the sampling points.

The samples collected from the first forest sub-catchment (BOU) are all clustered together, marked by higher concentrations for Al and Cd, and higher values for S1 compared to the other samples. Samples collected from the second forest sub-catchment (VRY) are also clustered together but show a different pattern, marked by higher concentrations of SiO_2. Samples collected at both grassland sub-catchments (VRN and REV) are well grouped despite their expected differences in terms of field capacity (Figure 1.B). They show high values for A1-254 and A2-254, indicating the presence of large organic matter molecules. Three of the five samples collected from the agricultural sub-catchment (PNC) are clustered, mostly characterised by higher concentrations of As and Co. Only one PNC sample is marked by high concentrations for the *rum-2-bac* DNA marker. Results show a good clustering for four COR samples representing the colluvium aquifer, marked by significantly higher

concentrations for a group of parameters including SiO_2, Li and Ba, in comparison to all other source samples. Among the five samples representing the colluvium aquifer (COR), two showed concentrations of human marker *Bacteroides* (HF183) higher than 6 $\log_{10}$ number of copies/100 mL (see concentration range in Table A6), close to the SEW samples concentration, taken directly from wastewater (median 7 $\log_{10}$ number of copies/100 mL). We considered that these samples were contaminated by wastewater, and removed them from the dataset. Three of the five wastewater samples (RES) are also well clustered and linked to a large group of parameters comprised of major ions (e.g. Na^+, K^+), dissolved metals (e.g. Pb, Cu, Zn), DOC and DOM indicators (A3-254). The urban and road runoff samples (PLR) show more variability as only three of the four samples are grouped and marked by high concentrations of V.

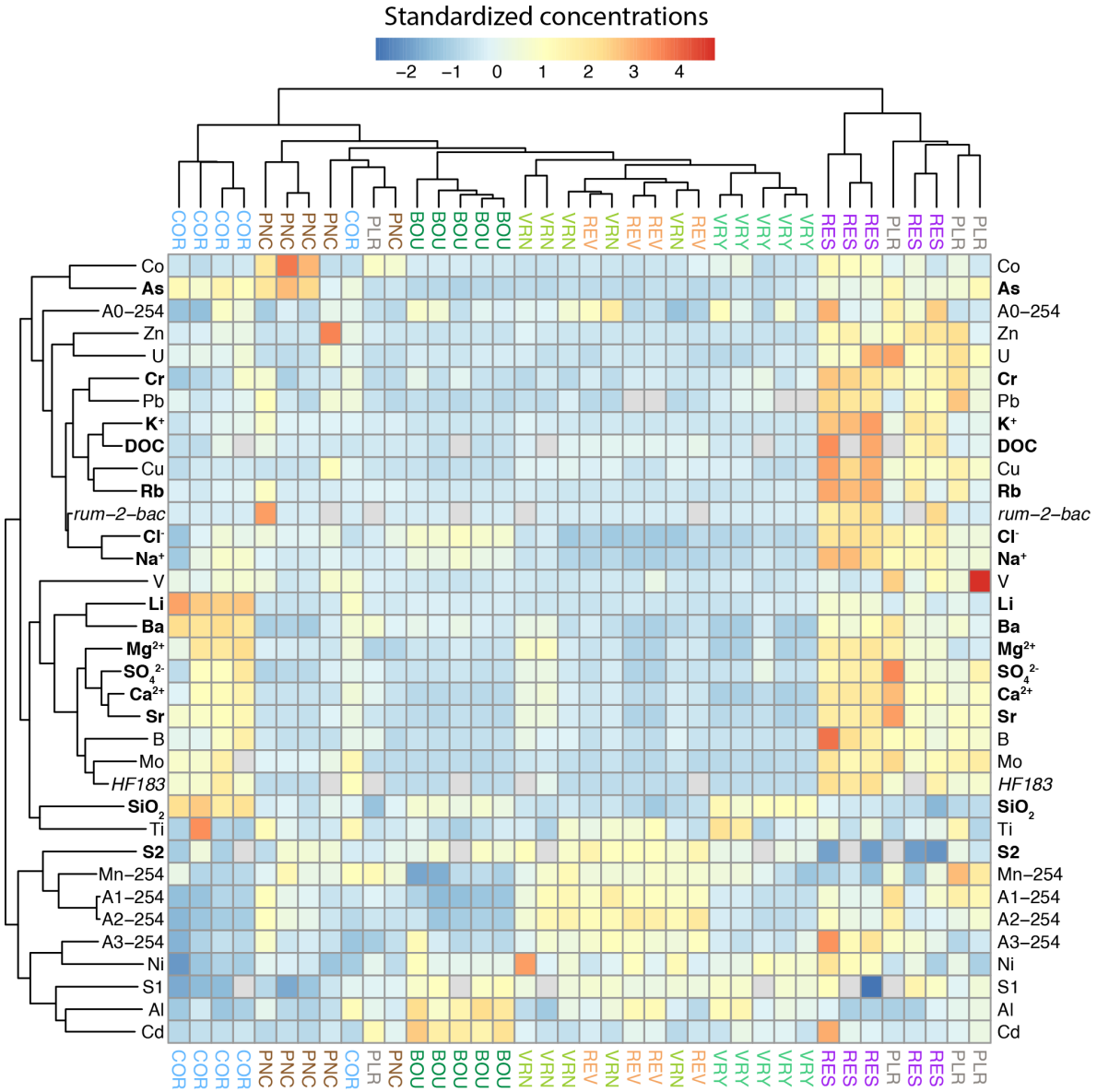

Figure 3 – Heatmap representation of the median concentrations of the biogeochemical parameters in samples from all selected sampling points. Standardised concentrations are shown in a range of colours from blue for negative values to red for positive values. Positive values represent high concentrations for a specific parameter and source sample, compared with the other samples. Negative values represent low concentrations for a specific parameter and source sample, compared with the other samples. Biogeochemical parameters and source samples are classified into groups based on Hierarchical Classification Analysis. Quick surface runoff (SUR) was not considered as all biogeochemical parameters were not available for this source. Bold parameters represent the final selection of tracer used in the Bayesian mixing model.

The differences between the BOU and VRY biogeochemical compositions do not suggest a unique biogeochemical signature associated to forest land use. Thus, we preferred to consider two different sources related to forest (FOR-1 and FOR-2). In contrast, we considered a single source associated to the presence of grassland, based on the clustering of the VRN and REV samples. Each of the remaining sampling points was considered as a distinct source. Table 1 shows the final typology proposed to describe the runoff-generating sources; it was used for the next step of the present study, including the new codes used to describe the nature of each source (AQU, FOR-1, FOR-2, GRA, AGR, SEW, URB and SUR).

3.2 Building-up the biogeochemical signatures

After discarding the parameters considered to be non-additive and non-conservative according to their nature, 33 parameters remained. Application of the range-test pointed out 13 other non-conservative parameters, with concentrations or values outside the range observed for the source samples, mostly concerning the HPSEC indicators and the dissolved metals Al and Co. The Kruskal-Wallis and Dunn tests showed two non-discriminant parameters: Ni and Ti with respective *p-values* of 0.06 and 0.93. Finally, the application of the LDA-Wilks lambda approach (Figure 4) showed that an optimal selection of 15 tracers was sufficient to discriminate the eight sources. These tracers correspond to seven major parameters (Cl^-, SO_4^{2-}, Ca^{2+}, Na^{2+}, K^+, Mg^{2+} and SiO_2), six dissolved metals (As, Ba, Cr, Li, Rb, Sr), and two DOM characteristics (DOC, spectral slope S2). These parameters were used to build the biogeochemical signatures of each source. We represented these signatures in Figure 5.

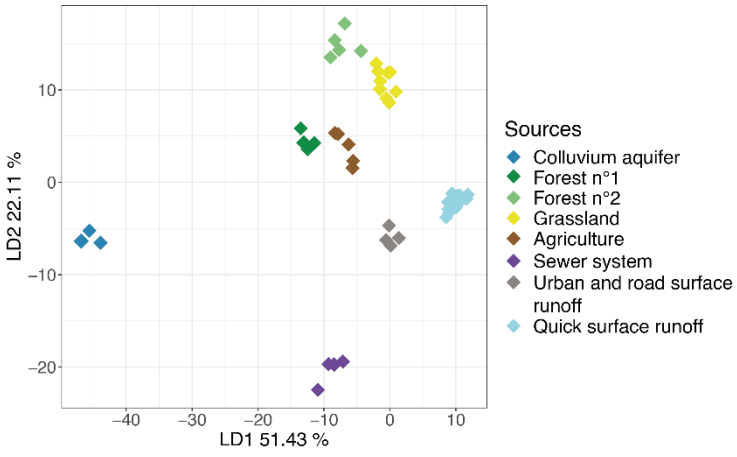

Figure 4 – Source samples coloured according to the sources identified and projected along the axes created by the Linear Discriminant Analysis. The concentrations used correspond to the optimal selection of tracers resulting from the selection by minimisation of Wilks' lambda.

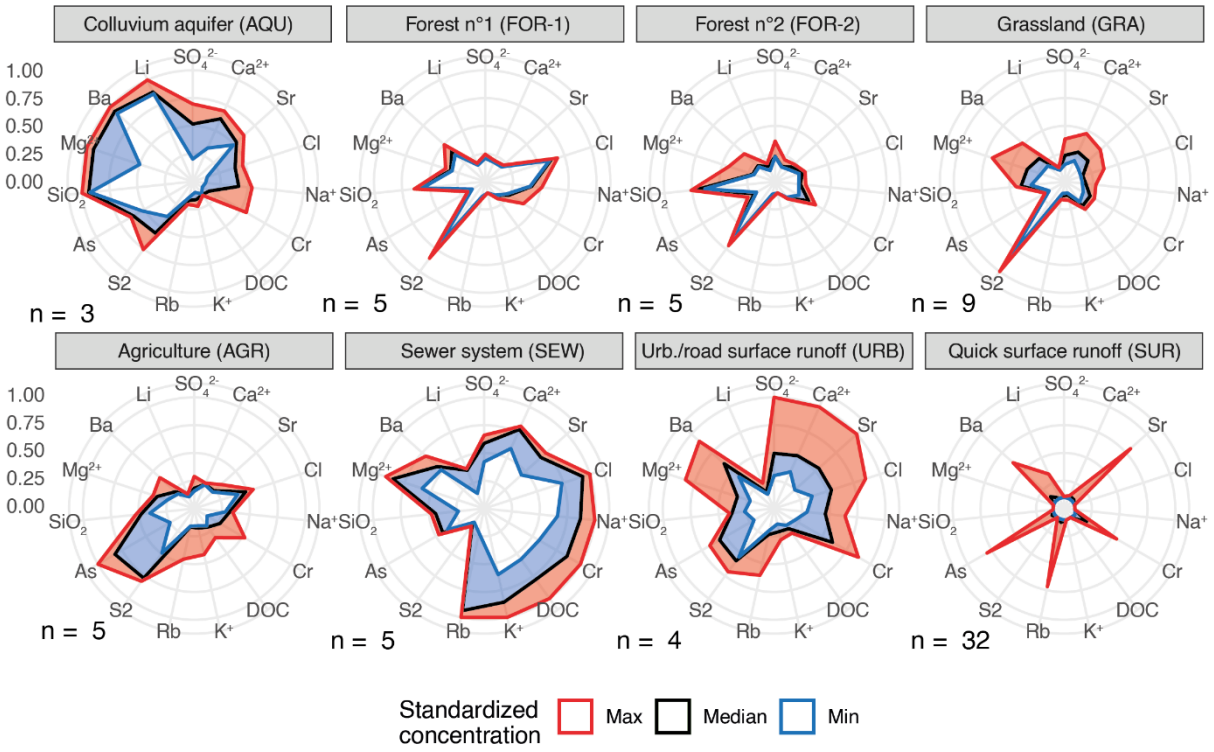

Figure 5 – Biogeochemical signatures of the identified sources, in the form of a radar plot. The 15 tracers correspond to the optimal selection resulting from the reductionist approach. Maximum, median and minimum concentrations are presented after standardization across all 15 tracers. n: the number of samples per source; Urb: urban.

The FOR-1 and FOR-2 signatures show low and stable concentrations, with high values of the parameter S2, which is a spectral slope calculated from absorption coefficients (350-400 nm), negatively correlated with the amount of aromatic carbon (Helms et al., 2008). The GRA signature is even more marked by high values of S2. Headwater from forests and grasslands is thus characterised by poorly aromatic DOM, which could be linked with high soil weathering (Wang et al., 2023). Boukra et al. (2023) showed similar results for surface waters from forest sub-catchments within the Ratier catchment, with a significant difference between water from forest watershed, less aromatic and water from agricultural areas (vineyards), more aromatic. Samples from the agricultural sub-catchment (AGR) also show higher values of the parameter S2, indicating low aromaticity, but are also characterised by even higher concentrations of the trace element As. According to Liu et al. (2020), significant concentrations of As can be observed in bovine manure, ranging from 2 to 17 mg/kg, which can explain the concentrations obtained for the AGR samples (median of 4.25 µg/L). The AQU signature is particularly characterised by high values of SiO_2,

364 Mg^{2+}, Ba and Li. Grandjouan et al. (2023) pointed out that this runoff generating source is mainly fed by a colluvium aquifer,
365 which significantly contributes to the Ratier stream volume outside of rainfall events, and attributed the high Li, Ba and Mg^{2+}
366 concentrations to a geological origin. High SiO_2 concentrations are often observed in groundwater (Iorgulescu et al., 2005).
367 The URB signature shows variable concentrations, with wide ranges, for SO_4^{2-}, Ca^{2+}, Sr, Cr, Mg^{2+} and Ba. This composition
368 can be explained by the leaching of urban soils during rainy events, leading to the release of the elements that could have been
369 emitted by urban and road pollutions sources and deposited at the surface of these soils. This phenomenon can be amplified
370 by a first-flush effect, which favours the transport of elements for the first rains after long periods of dry weather (Deletic and
371 Orr, 2005). The SEW signature is marked by high concentrations for Cl^-, Na^{2+}, Cr, DOC, K^+, Rb and Mg^{2+}, which is in line
372 with the classical composition of wastewater seen in the literature (e.g. Eme & Boutin, 2015; Fröhlich et al., 2008). The
373 variability observed for this source can be explained by the choice to collect the SEW samples during periods of rain (see
374 Section 2.2.1). Therefore, water samples from the SEW source consist of a mix of wastewater, rainwater and road surface
375 runoff, since this is a combined sewer network. Finally, the signature obtained for SUR shows very low concentrations for
376 most of the 15 tracers, with the exception of high maximum concentrations for Sr, Cr, Rb, As, Ba. According to Becouze-
377 Lareure (2010), these high concentrations are associated with atmospheric inputs to rainwater from the industrial Rhône valley,
378 in the south-east of the Ratier catchment.

379 **3.3 Hydrograph separation**

380 **3.3.1 Dry weather**

381 Figure 6 shows the relative contributions estimated for the 24 streamwater samples collected at the Mercier and Ratier outlets
382 outside from rainfall events. Figure A1 represents the equivalent contributions in daily volumes (in m^3) that we calculated
383 considering that the discharge measured at the time of sampling was representative of the daily discharge. Results for the
384 Mercier catchment showed little seasonality with similar results between low and high flow. The AGR source contributed the
385 most at low flow (up to 40% of total runoff) and the GRA source at high flow (up to 50%). The SEW contribution was
386 significant at both low and high flow conditions (between 10 and 50%), despite the absence of sewer overflow devices within
387 the Mercier catchment. We estimated median volume contributions of wastewater close to 30 m^3/day at low flow and
388 800 m^3/day at high flow. As a comparison, Dubois et al. (2022) estimated the average daily wastewater flow from a French
389 household around 0.311 m^3/day, and Aussel et al. (2004) the wastewater discharge per inhabitants in France around 0.2 m^3/day.
390 Wastewater contribution to the Mercier stream therefore represents the equivalent of a contribution of 100 households or 150
391 inhabitants.
392 Results for the Ratier catchment show a significant influence of the AQU source with a high seasonality. Contribution of AQU
393 was predominant at low flow, up to 85% of total runoff (more than 500 m^3/day). At high flow, although the estimated daily
394 volume for groundwater was higher than low flow (around 2 000 m^3/day), the relative contribution was lower (around 20%).
395 It was diluted by the other sources, such as GRA, which showed a major relative contribution (between 30 and 50%). The

relative contributions estimated for SEW were lower than for the Mercier station (below 10%), but the volume contribution remained stable (around 30 m^3/day at low flow and 1 000 m^3/day at high flow).

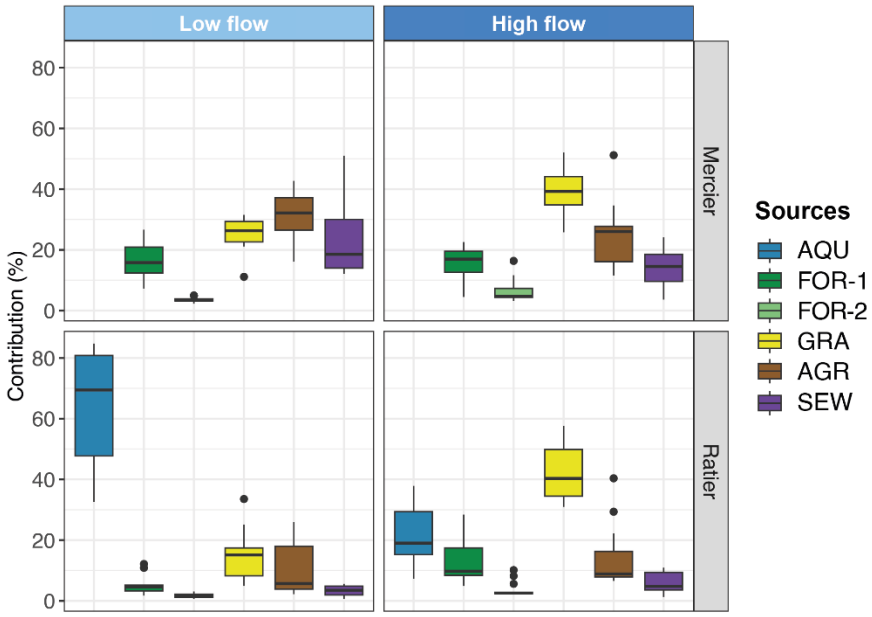

Figure 6 – Sources contribution to runoff estimated for dry weather samples by the application of a biogeochemical decomposition using a Bayesian mixing model for the Mercier and Ratier catchments. Boxplots represent the median contribution, interquartile range (1st and 3rd quartiles), minimum and maximum values. Low flow samples correspond to a mean daily discharge lower than 20 L/s and high flow samples to a mean daily discharge higher than 20 L/s.

3.3.2 Hydrological events: mean contributions

Figure 7 shows the mean of the source contributions estimated for each sampled hydrological event. We calculated these means from the individual results obtained by the application of the Bayesian mixing model on each streamwater sample (10 to 12 by event, see Section 2.2.2). Figure 7 also illustrates the uncertainty obtained for each event, in the form of the mean of the standard deviations obtained by applying each Bayesian mixing model decomposition, calculated from the sum of the squares of each deviation. Further results are detailed below as the mean with associated uncertainty (noted as *s.d.* for standard deviation). Figure A2 represents the contributions of each event in total volume, calculated based on the relative contributions for each source and the total flow in m^3.

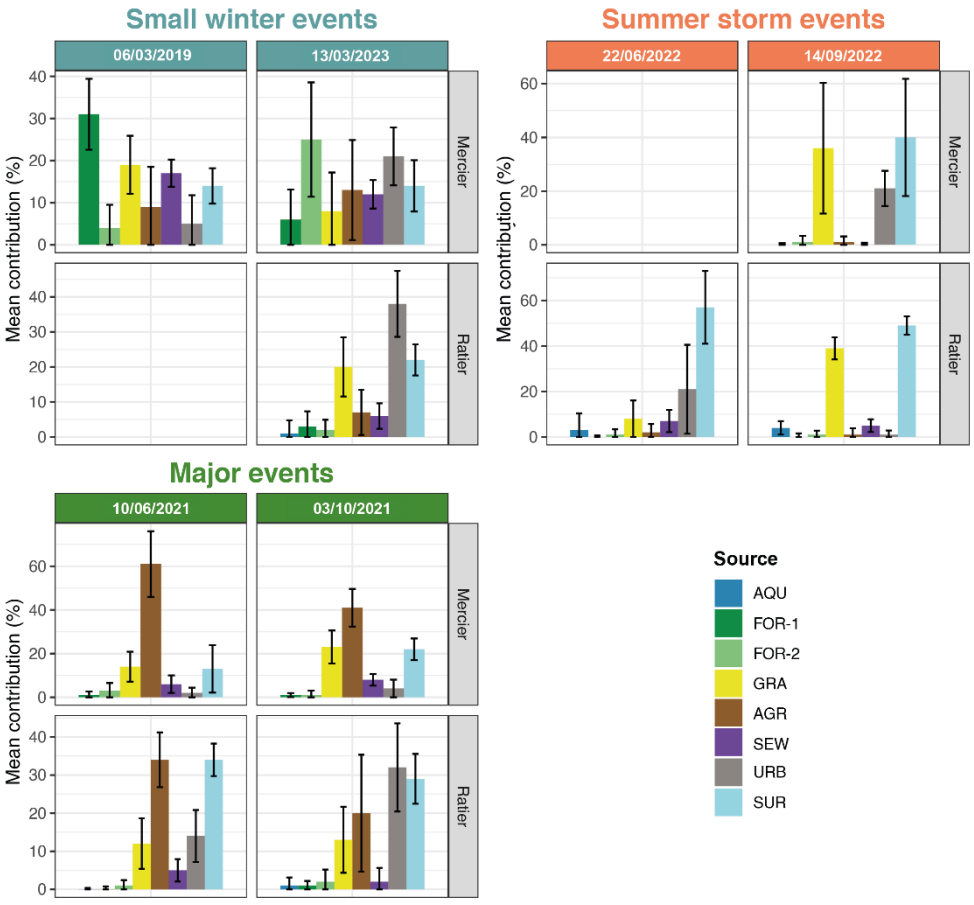

Figure 7 – Mean source contributions to the hydrological events sampled between March 2019 and March 2023 at the outlets of the Mercier and Ratier catchments. The contributions correspond to the mean of the results obtained for each sample decomposition by the Bayesian mixing model. The error bars correspond to the mean of the standard deviation calculated from the sum of the squares of the deviation. The events of 6 March 2019 at the Ratier station and 22 June 2022 at the Mercier station were not collected.

Results for small winter events show contrasted contributions. At the Mercier station, the major contribution was FOR-1 in March 2019 (31%, *s.d.* 8%). The FOR-2 source was the major contribution in March 2023 (25%) but with relatively high uncertainty (*s.d.* 14%). These contributions remained higher than those estimated at the Ratier station for both forest sources (5% in total; 3 and 2 %, *s.d.* 4 and 3%, respectively), which is consistent with the results obtained for dry weather. The contributions of URB were significantly higher for the March 2023 event than for the March 2019 one, with 21% (*s.d.* 7%) at the Mercier station and 38% (*s.d.* 9%) at the Ratier station. This contrast can be explained by three times more rain in March 2023 (18 mm) than in March 2019 (7 mm). The source SEW showed high contributions at the Mercier station, similar to those estimated for dry weather (17 and 12% respectively for March 2023 and March 2019; with low uncertainty, *s.d.* 3% for both events).

Results for the summer storm events showed predominant contributions of GRA, URB and SUR (>40%), but with higher uncertainties for the September 2022 event at the Mercier station (*s.d.* 24%, 7% and 22%, respectively) compared to the Ratier station (*s.d.* 5%, 2% and 4%, respectively). The URB contribution for the September 2022 event was lower at the Ratier (1%, *s.d.* 1%) than at the Mercier station (21%, *s.d.* 7%), despite a higher urban spatial extent at the Mercier catchment. We calculated high contribution of URB for the June 2022 event at the Ratier station (21%), but associated to high uncertainty (*s.d.*, 20%).

Results for both major events showed predominant contributions for AGR: 61% (*s.d.* 15%) and 41% (*s.d.* 9%) at the Mercier station, 34% (*s.d.* 7%) and 20% (*s.d.* 15%) at the Ratier station. Uncertainty of the results were relatively low, with the exception of the October 2021 event at the Ratier station. We calculated significant SUR and URB contributions at the Ratier station, but with higher uncertainties for the urban source: 14% *(s.d*. 7%) and 32% (*s.d.* 12%) for URB, 34% (*s.d.* 4%) and 29% *s.d.* 7%) for SUR. The SUR and URB contributions estimated at the Mercier station were lower (<4% for URB and <22% for SUR), despite the high rainfall recorded for these events (92 and 89 mm). The relative contributions estimated for SEW were low, but showed high wastewater volumes when related to the total flow volume observed for each event. We estimated SEW volume flows around 900 and 2 000 m^3 at the Mercier and Ratier stations, respectively, during the May 2021 event, and around 1 000 m^3 for both stations during the October 2021 event (Figure A2). Such volumes of wastewater transferred to the stream are equivalent to the mean daily wastewater discharge for 3 000 to 6 500 French households, or for 5 000 to 10 000 inhabitants (Aussel et al., 2004; Dubois et al., 2022).

3.3.3 Hydrological events: temporal variability of contributions

Figure 8, Figure 9 and Figure 10 present the decomposition results for the small winter events, the summer storm events and the major events, respectively. They illustrate the temporal variability of the estimated contributions for each source. These results and the associated uncertainties are detailed for each sampling time in Table A7, Table A8 and Table A9.

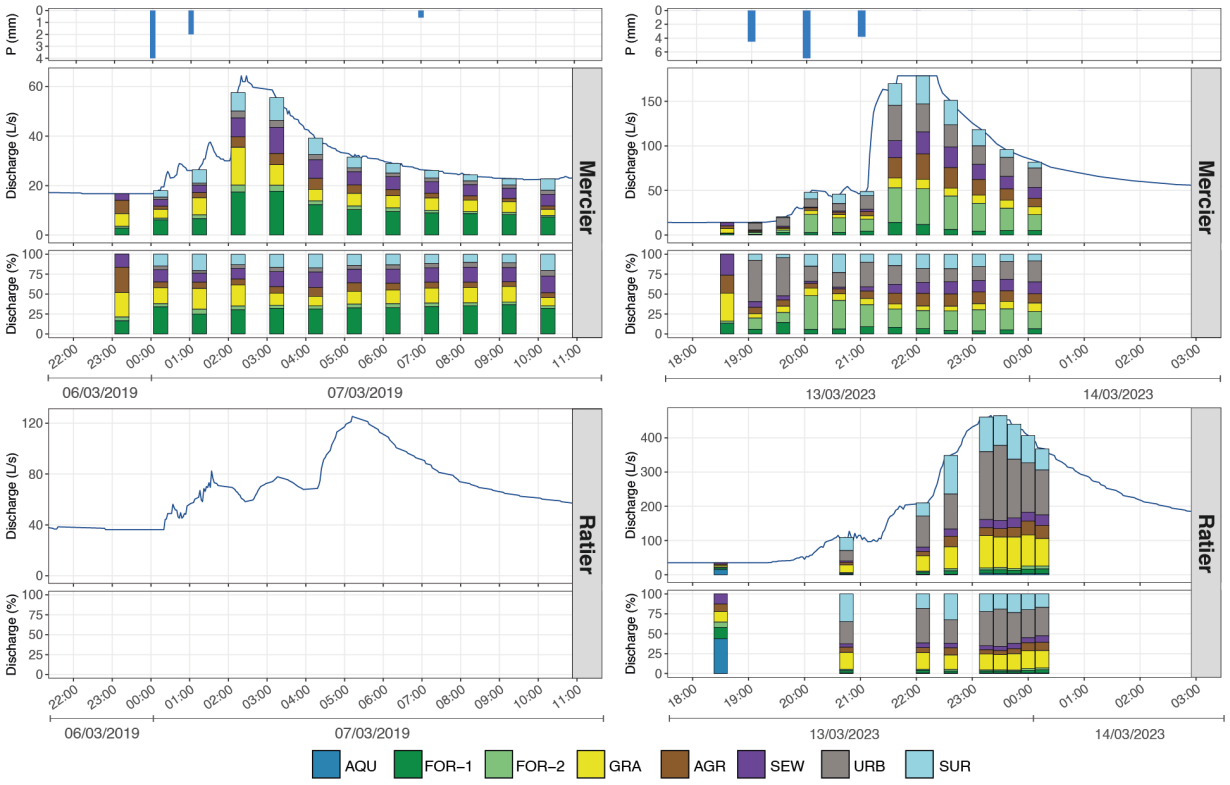

Figure 8 – Precipitation and hydrograph separation results for the sampled events at the Mercier and Ratier stations for the small winter events of March 2021 and March 2023. The upper parts show bars whose sizes correspond to the instantaneous discharges (in L/s) associated to the decomposed samples. The lower parts show stacked the relative contributions in a range from 0 to 100%.

For the two small winter events of March 2019 and March 2023 (Figure 8), the first sample was taken before the arrival of the rain. The contributions obtained for these samples prior to rainfall are consistent with the contributions estimated for samples collected under dry weather conditions: the contribution of FOR-1 was around 15%, that of GRA around 30%, and that of AQU around 44% (*s.d.* 11%). However, results for FOR-1 and GRA are associated with relatively high uncertainties (*s.d.* 10 to 11% for FOR-1 and 1 to 23% for GRA). As for dry weather results, the contribution of SEW was higher on the Mercier (up to 26%, *s.d.* 4 to 5%) than on the Ratier (13%, *s.d.* 7%). These results confirm the estimations obtained for dry weather. These contributions changed once the rain started, but remained stable until the end for each small winter event, despite the evolution of discharge. All these contributions estimated during rainfall were very close to the mean contributions shown in Figure 7. The contribution of urban and road surface runoff in March 2023 for the Ratier was the largest, right from the start of rainfall (52%, *s.d.* 7%), which might suggest particularly localized rainfall in urban areas. The contribution of the sewer system remained stable over the March 2019 event for the Mercier, showing a rising input of wastewater into the stream proportional to the total discharge. For the March 2023 event, the contribution of the sewer system decreased during rainfall, suggesting a dilution of wastewater by rainwater in the sewer system.

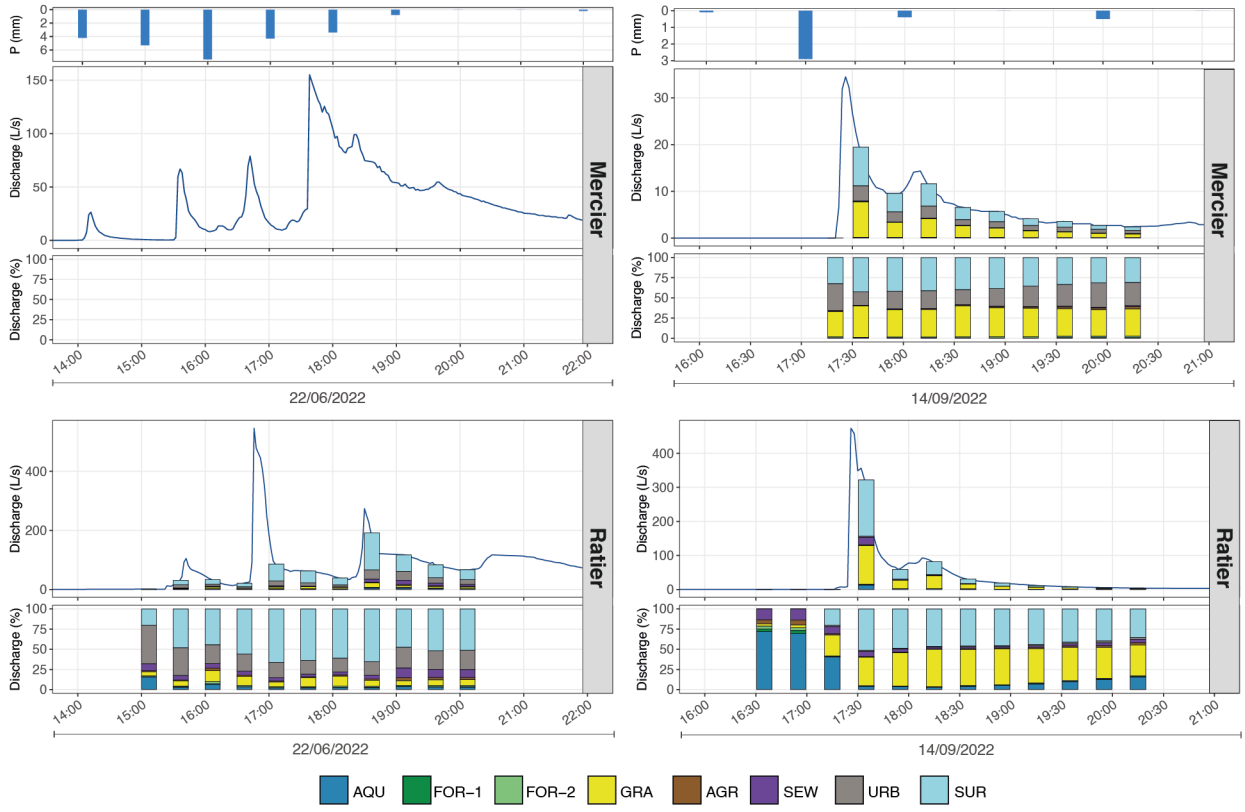

Figure 9 – Precipitation and hydrograph separation results for the sampled events at the Mercier and Ratier stations for the summer storm events of June 2022 and September 2022. The upper parts show bars whose sizes correspond to the instantaneous discharges (in L/s) associated to the decomposed samples. The lower parts show stacked the relative contributions in a range from 0 to 100%.

For the two summer storm events, most of the contributions remained relatively stable (Figure 9). The quick surface runoff (SUR) contributions remained the largest and the most variable ones. The estimated contributions for this source varied widely for the Ratier (from 20 to 65%), but were more stable for the Mercier (from 30 to 40%). However, uncertainties were lower for the Ratier (*s.d.* between 9 and 23%), than for the Mercier (*s.d.* between 17 and 28%). The largest contributions for the Ratier were estimated during peak flows with relatively low uncertainty (max 65% for the June 2022 event, *s.d.* 15%; and 50% for the September 2022 event, *s.d.* 4%). The estimated contributions from the sewer system (SEW) also varied along the events for the Ratier: from 3 to 12% (*s.d.* from 3 to 7%) in June 2022 and from 2 to 14% (*s.d.* from 1 to 6%) in September 2022.

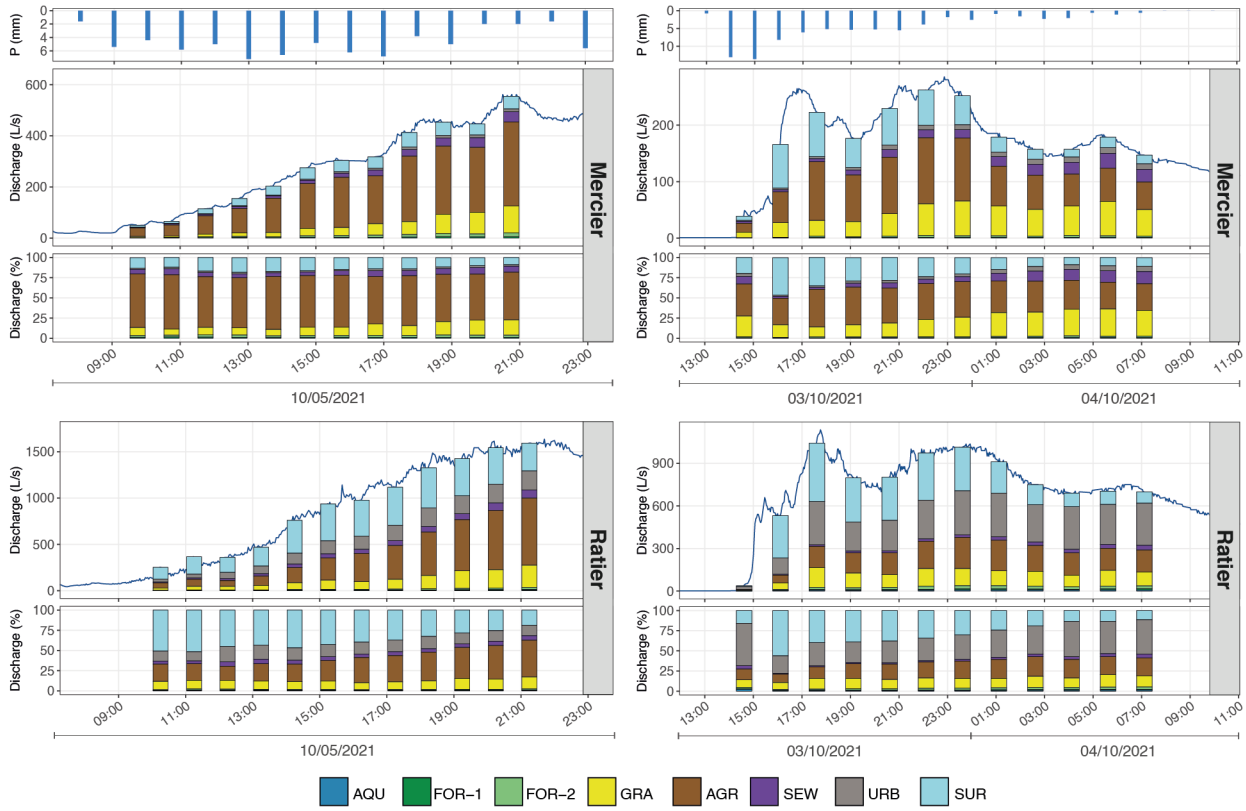

Figure 10 – Precipitation and hydrograph separation results for the sampled events at the Mercier and Ratier stations for the major events of May 2021 and October 2021. The upper parts show bars whose sizes correspond to the instantaneous discharges (in L/s) associated to the decomposed samples. The lower parts show stacked the relative contributions in a range from 0 to 100%.

Finally, the contributions estimated for the two major events also showed relatively low temporal variability (Figure 10). The predominant contribution was from agricultural areas (AGR), which varied from 33 to 66% for the Mercier (*s.d.* from 8 to 17%), and from 10 to 45% for the Ratier. The AGR contributions at the Ratier showed higher uncertainties for the October 2021 event (*s.d.* from 9 to 20%) than for May 2021 event (*s.d.* 4 to 11%). The contribution of quick surface runoff showed higher variability, particularly for the event of October 2021, with a predominant part during the peak flow (47% for the Mercier, *s.d.* 6%, and 5% for the Ratier, *s.d.* 6%). For the May 2021 event, the quick surface runoff contribution never represented the majority. The contribution of wastewater was stable for the Ratier (around 5%, *s.d.* from 2 to 7%), but increased significantly for the Mercier (up to 15%, *s.d.* from 1 to 4%).

4 Discussion

4.1 Questioning the representativeness and nature of the sources

The application of a mixing model for decomposition of streamflow implies that the sources are well represented by their biogeochemical signatures. In the present study, these signatures were particularly well defined for forests and grasslands. The signature of the colluvium aquifer (AQU) was more variable, but remained significantly marked by high concentrations of Li, Ba and SiO_2 in all the samples. However, the concentrations of human-specific faecal markers measured in several AQU samples confirm a contamination of the colluvium groundwater by wastewater. The signatures for other sources showed much more variability (Figure 5). Our results question the representativeness of these signatures and the initial assumptions on which the identification and sampling of these sources were based.

Defining the biogeochemical signatures of agricultural sources based on a single sub-catchment turned out to be challenging and highlighted three main difficulties. First, the catchment's characteristics made it difficult to delineate homogeneous sub-catchments associated with specific agricultural activities (e.g. crop culture, bovine breeding). Second, observing even a small flow at the outlets of agricultural sub-catchments was challenging due to the small size of these catchments and the predominance of crops and grasslands, which are linked to lower field capacity. Under such conditions, infiltrated rainwater is either rapidly evapotranspired or percolated towards the underlying fractured gneiss, resulting in little or no observable discharge at the sub-catchment outlet. As a result, only one agricultural sub-catchment could be identified and sampled. Third, the nature and intensity of agricultural activities can vary from one year to the next, and even within a single year, leading to seasonal variations in the biogeochemical signatures. An example is the absence of ruminant-specific bacterial faecal marker (*rum-2-bac*) in 4 out of 5 PNC samples. This questions the use of qPCR as markers of source contributions, especially since microbial markers are strongly influenced by environmental factors like water temperature (Marti et al., 2017). The use of more specific and persistent tracers, such as organic micropollutants, could improve the identification and characterization of agricultural sources, in a more precise manner than the general tracers used in this study, which were selected for their simplicity (Grandjouan et al., 2023). Previous studies have explored alternative approaches. El Azzi et al. (2016) compared commonly used pesticides concentrations with results from a chemical mixing model in an agricultural catchment. In doing so, they established a link between specific pesticides and vertical contributions (surface runoff, subsurface runoff and groundwater). Banned pesticides that have not been used for several years could also be used, as long-term storage often occurs in agricultural catchments (Sandin et al., 2018). Our study could benefit from this approach, specifying the contribution from the agricultural areas while taking into account and evaluating the vertical contributions estimated by Grandjouan et al. (2023) (i.e., saprolite flow, fractured gneiss flow and colluvium groundwater; see Section 4.3).

We chose to sample water from the sewer system during rainfall events, in order to characterize the biogeochemical signature of the water transferred to streamwater during overflows. However, our results show that the heterogeneous nature of these samples, being a mixture of wastewater and urban and road surface runoff, has a strong influence on the contributions estimated for the SEW and URB sources. The mixing model faces a first limitation as it is unable to distinguish wastewater alone from

urban and road surface runoff. Indeed, the SEW signature may have been diluted and influenced by the URB signature, which already showed a variable biogeochemical composition. As a consequence, we may have overestimated the SEW contributions during the events. Moreover, the results for dry weather conditions are less reliable, as only wastewater is released through leaks from the sewer system to the stream. Ideally, we should have built the wastewater signature using samples collected from the sewer system under dry weather conditions, to better distinguish the URB contributions from wastewater.

In the case of urban and road runoff (URB), the first flush effect, implying the leaching of urban soils which favours high concentrations of contaminants (e.g. Cu, Pb, Zn) after longer dry periods (Deletic and Orr, 2005), makes it difficult to characterise a proper and unique signature. Indeed, Simpson et al. (2023) characterised the runoff water quality from 13 urban watersheds using classical tracers (i.e. nutrients, total suspended solids and metals), but showed that the pollutant concentration depended on the rainfall intensity, and that a first flush effect was not systematically observed. Innovative tracers could help characterising this source, as showed by Lin et al. (2024) who used DOM characteristics (with a fluorescence excitation-emission matrices spectroscopy technique) to estimate the contribution of road runoff in an urban catchment. They found that the water generated by road runoff exhibited high aromaticity of DOM. In the present study, the values of the DOM parameter S2, which is negatively correlated with aromaticity, were indeed lower for the URB signature than for the other sources. Hence, we confirmed the usefulness of using such DOM characteristics as tracers in a mixing model.

Finally, as the quick surface runoff (SUR) composition was inferred from rainwater composition, it may be more or less distant from reality. The hypothesis of a quick surface runoff keeping the biogeochemical signature of rainwater is questionable as these waters can quickly accumulate elements (Langlois and Mehuys, 2003). Yet, Fröhlich et al. (2008) conducted a similar study in the Dill Catchment (Germany), aimed at identifying runoff sources, including wastewater, groundwater and stormwater flow, in which they grouped surface and subsurface runoff. To do this, they sampled streamwater from the outputs of sub-catchments characterized by specific geological formations, during baseflow and hydrological events. They showed that the geochemical composition of stormflow was similar to the composition of precipitation, characterised by low-mineralization. Their results suggest the predominant contribution of low-mineralized waters for several events, which support the use of the composition of rain to represent the quick surface runoff source, in cases where runoff water could not be sampled. In any case, our study could benefit from a proper sampling of quick surface runoff in order to better estimate their contributions to streamwater. Several studies analysed direct surface runoff water collected on soil surface during hydrological events. Le et al. (2022) and Omogbehin & Oluwatimilehin (2022) both showed high concentrations of DOC transferred from soils to the stream by overland flow. Omogbehin & Oluwatimilehin (2022) also showed low-mineralised composition of the direct surface runoff water sampled. However, these two studies were conducted in a tropical area, where direct surface runoff often occurs outside of urban areas. Such sampling appears to be difficult in temperate areas, with less intense rainfalls.

Another method to characterise sources is the use of stable isotopes (e.g. $\delta^{2}H$, $\delta^{18}O$). While many studies have used isotopic tracers in mixing models to estimate the contributions from different runoff-generating sources, few of them were applied to peri-urban catchments with complex land use distributions. Kuhlemann et al. (2021) estimated the contribution of wastewater in the Erpe peri-urban catchment (Germany) using isotopic tracers together with physico-chemical parameters of water (i.e.

conductivity and temperature of water), in an Bayesian mixing model (using MixSIAR). However, they also faced high uncertainties due to the similarities in concentrations between the composition of wastewater and other runoff sources. They concluded by recommending the use of both isotopic and geochemical tracers to overcome these limitations.

4.2 Evaluating the estimated source contributions

Our results showed contrasted contributions from the different sources in the catchments, that were also variable in time according to the meteorological conditions. A possible explanation for this could have been that runoff contributions from a specific source are proportional to its spatial extent within the catchment, but this hypothesis is invalidated by our results. Several additional factors to spatial extent appear to influence source activation and the hydrological response of the catchments, as described below.

Contributions of the colluvium aquifer was constant, regardless of the hydro-meteorological conditions, as already shown by Grandjouan et al. (2023).

Forests, that represent 30 to 38% of the Ratier and Mercier catchments (Table A1), contributed to approximately 30% of total runoff in dry weather conditions (Figure 6) and for small winter events at the Mercier outlet (Figure 7). However, these contributions were much lower at the Ratier outlet and negligible for summer storm and major events (Figure 7). The major contribution of forests to the Mercier stream during small winter events, and the fact that we sampled the two forest sources at every campaign, independently from the hydro-meteorological conditions could be explained by the geological characteristics of the upper part of the catchment. The saprolite horizon being thin in this area, it cannot store a large volume of water. Alternatively, the constant flow generated by these springs may originate from the fractured gneiss, fed by infiltrating rainwater. Recharge water can have a piston effect, pushing the groundwater retained within the fractures towards the stream. Lachassagne et al. (2021) described a similar behaviour on another catchment characterised by fractured crystalline formations and thin saprolite layer with (1) a vertical piston effect in the saprolite layer and (2) a preferential deep horizontal flow in the fractures of the basement. During summer period, the minor forest contribution can be linked to the favoured retention of rainwater by the vegetation over runoff (Bruijnzeel, 2004).

Grasslands and agricultural lands together account for approximately 50% of the Mercier and Ratier catchments (Table A1), but were associated with highly variable contributions at the outlet of both catchments and depending on the different type of events (Figure 7). These variations can be explained by the highly variable thickness of the saprolite horizon downwards from forest - 1 to 20 m according to Goutaland (2009). The absence of runoff for the GRA and AGR sources under low flow conditions and dry weather suggests the existence of throughs at the saprolite-gneiss interface in which water can be stored and released discontinuously. This process was described as “fill-and-spill” by McDonnell et al. (2021), and observed in the Panola catchment by Tromp-van Meerveld & McDonnell (2006), and in the Pocket lake catchment by Spence & Woo (2003), both being characterised by a similar crystalline bedrock. They showed that the generation of subsurface and surface flow in this context can be delayed, as it requires to meet sufficient rainfall amount to increase water storage at the soil-bedrock boundary. When these conditions were not observed, Spence & Woo (2003) and Tromp-van Meerveld & McDonnell (2006)

noticed intermittent flow, which is similar to what was observed in the Mercier and Ratier catchments. Indeed, contribution from agricultural lands are low or absent during summer storm events, and dominant during major events, when rainfall amounts were sufficient. However, grasslands showed quicker and more frequent responses in wet weather conditions. This difference may be linked to lower interception by vegetation, shallower root systems, and reduced water demand in grasslands compared to forests or crops (Madani et al., 2017; Robinson and Dupeyrat, 2005).

Our results also show that summer storm events are often associated with the generation of quick surface runoff. Indeed, Shi et al., (2021) showed that low antecedent soil moisture during summer periods can enhance the generation of quick surface runoff. The lower general evapotranspiration demand from grassland may also favour the quick surface runoff for this particular land use. As seen in Section 4.1, DOC can easily be transferred from soils to runoff water. As a consequence, the quick surface runoff contribution generated at the surface of grasslands could also have been considered as grassland contribution by the mixing model. These results suggest that both vegetation type and antecedent soil moisture influence the likelihood of quick surface runoff generation.

The high contributions of SEW to the Mercier streamwater suggest continuous wastewater inputs, either from sewer leakage or from non-collective sanitation. At the Ratier, similar wastewater volumes were observed but diluted by larger baseflow. Grandjouan et al. (2023) already showed that the sewer system has a strong influence on streamwater in dry weather conditions, as they measured high concentrations for the *HF183* human-specific faecal markers in both Mercier and Ratier streams (mean values of 2.4 and 2.5 $\log_{10}$ copy nb/100mL, respectively). Tran et al. (2019) observed a similar trend in agricultural areas with low residential and urban extent, with runoff water composition similar to the composition of raw wastewater. They also suggest that these contributions come from leaks from the sewer system. In the present study, during hydrological events, the increase of wastewater contributions can be explained by sewer overflows, occurring both at the combined sewer overflow device and at other points of the network. According to local sewer network managers, such overflows are frequent even during small winter events (<10 mm), due to undersized sewer infrastructure. Such wastewater transfer remains difficult to characterise in terms of both dynamics and volume. Numerical modelling of the sewer leakage and overflow appears to be a promising way of quantifying these impacts on groundwater (Nguyen et al., 2021).

Mean contributions from urban and road runoff were estimated with high variations according to the different types of events, and subject to high uncertainty. These uncertainties can be explained by the difficulty for the mixing model to distinguish wastewater from urban runoff (see Section 4.1), which may have influenced our calculations. The presence of the sewer system has a major influence on these contributions, due to the loss and gain of urban and road runoff water through the presence of storm drains and sewer overflow devices. Another factor that could have influenced the URB contributions is the spatial rainfall variability, for example during the September 2022 event where the Mercier showed higher URB contribution compared to the Ratier, despite being less urbanised. Rainfall recorded at the pluviometric stations across the Ratier catchment were indeed highly variable during this event, ranging from 8 mm at the La Croix du Ban station to 37 mm at the Pollionnay station, with an intermediate value of 14 mm at the Col de la Luère station (Figure 1.D; Lagouy et al., 2022). This is particularly relevant during convective summer storm events, where precipitations are localised and lead to quick response of urban areas, as

showed by Kermadi et al. (2012) for the Yzeron catchment (which includes the Ratier catchment). The influence of rainfall spatial distribution on hydrological response in urban areas is undergoing increasing study, especially through hydrological modelling (Cristiano et al., 2017). Such studies encourage the use of high spatial resolution radar weather radar images for studying rainfall spatial variability in small peri-urban catchments, although this remains uncommon (Emmanuel et al., 2012). Overall, these findings emphasize the role of the geological characteristics, water storage capacity, vertical flow transfer, variations in water transit time, and specific losses or gains associated to the sewer system, in addition to land use diversity.

4.3 Improving the hydrological perceptual model of the Ratier and Mercier catchments

Grandjouan et al. (2023) built an initial perceptual hydrological model of the Ratier catchment, describing the general hydrological behaviour of the catchment and the main contributions to streamflow. That model was based primarily on dry-weather observations; it identified three main sources including colluvium groundwater, fractured gneiss groundwater and the saprolite layer. The authors reported positive correlations between discharge and saprolite contribution, and negative correlations between discharge and gneiss groundwater contribution. However, they also showed unclear boundaries between both contributions, and suggested that land use could play a stronger role than geology in runoff generation. The extensive dataset obtained in the present study, together with the insights gained from results presented in Sections 4.1 and 4.2, improves the initial representation of the catchment hydrological behaviour by Grandjouan et al. (2023). Figure 11 shows the new hydrological perceptual model proposed for the Ratier and Mercier catchments. It represents the hydrological dynamics of each identified source that were consistently supported both by the results of the present study and literature.

In order to simplify the model, we chose to merge the two forest sources FOR-1 and FOR-2 as they represent similar areas of the catchment. These sources are characterised by a shallow or absent saprolite depth, with the fractured gneiss formation sometimes outcropping. The dominant process is groundwater contribution from fractured gneiss, recharged by rainfall and mobilised through a piston effect. Contributions of forest is therefore considered stable in baseflow conditions, a little higher during small winter events and much higher during storm events. During summer storms, forest contributions remain minor due to strong canopy interception and high evapotranspiration. For grasslands, generation of runoff is generally driven by a fill-and-spill mechanism within the saprolite layer, producing intermittent sub-surface contributions. Hence, the contribution from grasslands strongly depends on the topography of the saprolite-gneiss boundary. In wet weather conditions, grasslands also generate rapid surface runoff due to low canopy interception and lower evapotranspiration. For agricultural lands, the same geological context suggests fill-and-spill dynamics, but contributions diverge from grasslands because of higher crop evapotranspiration. Their role appears to be minor in summer storms but can increase during major events. The sewer system contributes wastewater continuously through leakage and sanitation losses. These contributions are especially marked in the Mercier catchment. Episodically during hydrological events, a mixture of wastewater, urban and road surface runoff and rainwater is transferred to the stream through sewer overflows. The urban and road surface runoff contributions vary considerably as they strongly depend on the urban area extent, on the presence of urban infrastructures that collect runoff water, and mostly on rainfall spatial variability. Finally, the colluvium aquifer provides a nearly constant contribution

663 regardless of hydrological conditions. Evidence of wastewater contamination indicates that this source is characterised by both
664 natural groundwater and anthropogenic inputs.
665 This revised perceptual model shows that runoff-generating sources are driven by both natural controls (geology, subsurface
666 storage, vegetation) and anthropogenic drivers (sewer leakage, urban runoff). The model confirms that land use and urban
667 elements (sewage system, impervious areas) exert a first-order control on hydrological responses.
668
669

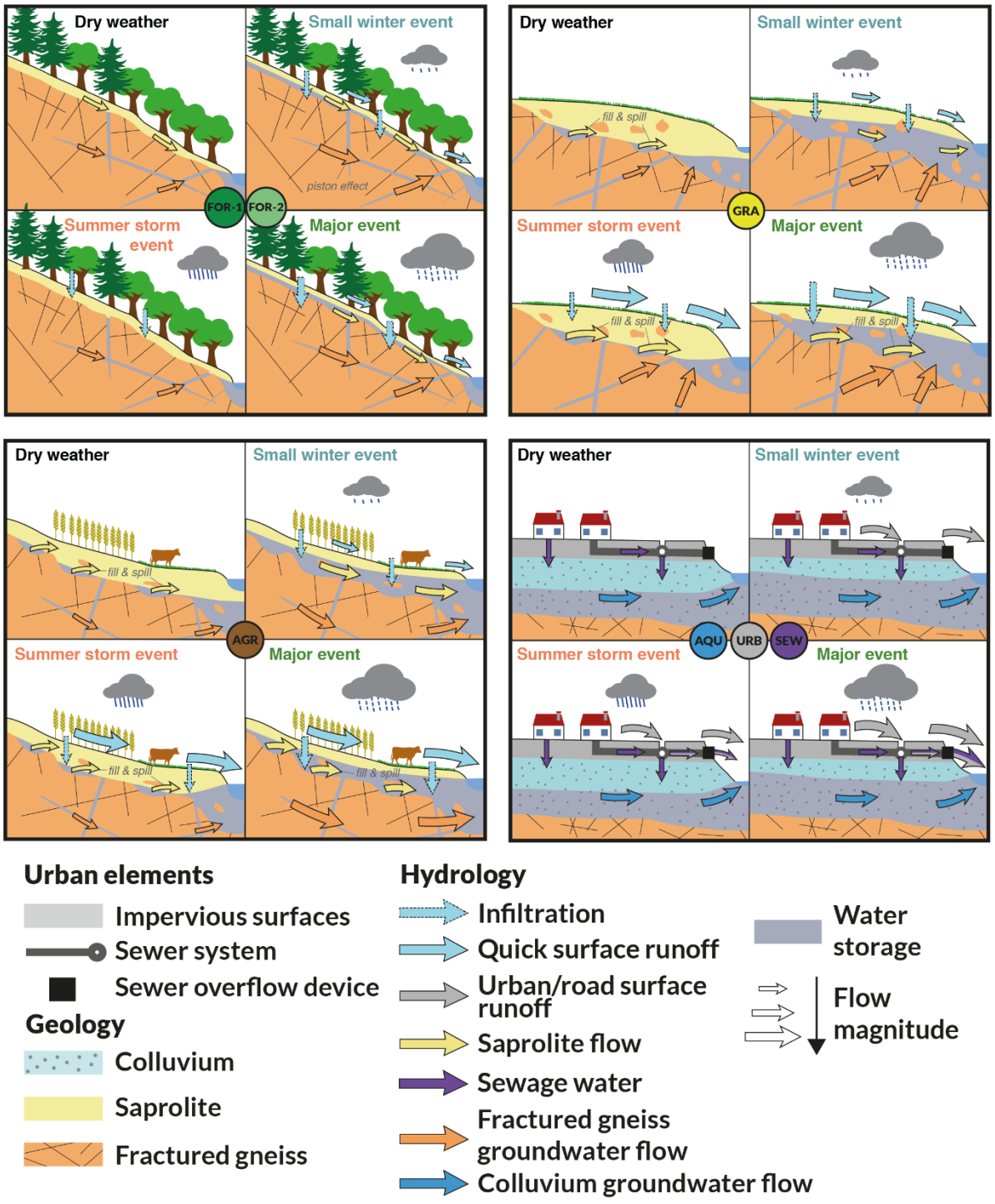

Figure 11 – Improved perceptual model of the Ratier catchment, initially build by Grandjouan et al. (2023). Main contributions, estimated by the mixing model, are illustrated according to the nature of the sources and the four hydro-meteorological conditions studied, including dry weather, small winter event, summer storm event, major event. FOR: forest; GRA: grassland; AGR: agricultural; AQU: aquifer; URB: urban and road surface runoff; SEW: wastewater.

4.4 Broader implications for hydrological understanding of peri-urban catchments

Beyond the specific results obtained for the Mercier and Ratier catchments, our findings and the updated perceptual model of the Mercier and Ratier catchments provide more general understanding of the hydrological behaviour of peri-urban catchments. Runoff generation and source activation appear to be strongly dependant not only on land use, but also on additional factors such as season, types of events, rainfall spatial variability, geological and pedological characteristics, and urban water infrastructures in the catchment. Our results show that, in addition to factors that control runoff generation, hydrological connectivity plays a key role in source contribution. Both "rural" factors classically taken into account in hydrology studies (soil, vegetation), and "urban" factors such as water management infrastructure must be jointly taken into account. In particular, our results indicate that the runoff contributions were not necessarily proportional to the spatial extent of their sources. Spatially limited and a priori disconnected sources such as urban areas and sewer systems, appeared to be highly connected and dominating streamflow composition and contaminant fluxes, despite their limited spatial extent.

We also showed that sewer systems and anthropogenic features can have a major impact on the quality of streamwater, even in low-urbanised and small headwater catchments. Groundwater in urbanised areas can be also considerably affected by anthropogenic contaminations, despite the theoretical hydraulic disconnection of the urban water system. These findings highlight the critical role of sewer system integrity in controlling streamwater quality, as system failures or leakages can facilitate transfers between wastewater, groundwater and surface water. This underlines the importance of having adequately designed, maintained and monitored sewer infrastructures. The persistence of wastewater inputs, even under low-flow conditions, highlights the specific vulnerability of peri-urban catchments, where poorly monitored and diffuse sources such as non-collective sanitation, can significantly impact streamwater quality.

Our findings have direct implications for the hydrological modelling of peri-urban catchments. We demonstrated that runoff contributions cannot be inferred only from the spatial extent of sources, as the area-weighted parametrisations, traditionally used in distributed hydrological model, may fail to represent the effective runoff-generating processes. Model structures and calibration strategies should instead account for hydrological connectivity, water management infrastructure, water storage capacity and transfer times, which jointly control source activation and streamflow composition. In addition, we highlighted the importance of including rainfall spatial variability as model input, even in small catchments such as the Ratier, particularly in peri-urban environments where convective events can lead to highly localised responses.

More broadly, modelling of peri-urban catchments hydrology can strongly benefit from the use of biogeochemical tracers such as major ions, trace metals and DOM characteristics. These tracers are relatively cheap and easy to analyse, and provide valuable information to identify and discriminate runoff-generating sources. When combined with Bayesian mixing models, they offer significant added value by improving the estimation of spatial source contributions and highlighting dominant water pathways. Distributed hydrological model could also benefit from this approach by providing an alternative means to evaluate simulated source contributions that are overwise difficult to validate using direct field observations. Overall, such approaches

can substantially improve the understanding of how land use, geological structures and hydro-meteorological conditions control streamwater composition and catchment hydrological behaviour.

5 Conclusions

The objective of this study was to identify runoff-generating sources in a small peri-urban catchment, and estimate their contributions to streamwater with a mixing model based on a biogeochemical dataset comprised of classical and original tracers. This approach showed the potential of the use of biogeochemical tracers to perform a spatial decomposition of water, based on the physical characteristics of a catchment, in addition to a more traditional vertical decomposition. Results showed that the use of indicators that are simple and cheap to analyse (major parameters, metals) together with more original tracers (DOM characteristics) was sufficient to differentiate each source according to geological, pedological and land use characteristics, or according to anthropogenic infrastructure. This study also showed the need for accurate methods to identify the runoff-generating sources and their biogeochemical signatures. An improvement of the approach would be a better characterisation of the most variable sources, such as agricultural lands, urban and road surface runoff and sewer system wastewater. Moreover, quick surface runoff needs to be collected and characterised to better estimate its contribution to streamwater. The initial campaign plan aimed to sample this runoff at various locations representing forest, grassland and agricultural areas. However, such sampling is challenging, as it requires being present at the right location and time due to the ephemeral nature of surface runoff. The deployment of automatic samplers could help overcome these limitations and improve data collection. Such sampling has already been implemented using a gutter-based collection system, as part of the ANR CHYPSTER project, in the Claduègne catchment (Ardèche, France).

This study demonstrated the effectiveness of the proposed method in estimating the water pathways and the main hydrological contributions in a peri-urban catchment. The mixing model provided reliable estimates for several source contributions. Confidence in the results was reinforced by the use of additional tracers beyond those used in the mixing model, such as DOM characteristics, microbial parameters and other dissolved metals. The results obtained with the mixing model were consistent with the initial perceptual hydrological model built for the Ratier catchment, and allowed us to build an improved version at the hillslope scale. This new perceptual model provides a better understanding of the behaviour of these two nested catchments and their hydrological dynamics depending on hydro-meteorological conditions.

More broadly, the application of mixing models in relation to land use remains relatively unexplored in the literature. This study highlights the potential of such an approach when incorporating biogeochemical parameters and highlights the need for further research in this direction.

This work illustrates the broader potential of mixing models to identified the spatial origin of streamflow and improve our understanding of catchment hydrological behaviour. Such approaches could provide valuable insights for validating spatially distributed hydrological models, which often face difficulties in adequately representing source contributions. More generally, combining mixing models with land use and hydro-meteorological data may help to better anticipate the impacts of land

management or climate change on runoff-generation processes. Future research should therefore focus on integrating tracer-based source characterisation with modelling frameworks, to improve both process representation and predictive capacity in peri-urban catchments.

Appendix

Table A1 – Combinations obtained from the superimposition of factors describing sub-catchments (geology, field capacity, land use). The relative surface areas associated with each combination is provided for the Mercier and Ratier sub-catchments. Combinations with a relative area of less than 1% of the Ratier catchment are not detailed.

Geology	Field capacity	Land use	Agricultural activity	Surface (%)	
				Mercier	Ratier
Gneiss	Low	Forest		0	1
		Agriculture	Unspecified	0	3
			Bovine breeding	0	2
		Urban		0	5
	Medium	Forest		30	20
		Agriculture	Unspecified	20	6
			Permanent grassland	5	6
			Bovine breeding	0	3
			Cereal crop	2	5
			Equine breeding	0	1
		Urban		5	11
	High	Forest		0	4
		Agriculture	Unspecified	14	4
			Permanent grassland	1	3
			Bovine breeding	6	4
			Cereal crop	1	2
		Urban		0	2
Colluvium	Medium	Urban		0	3

Table A2 – Limits of quantification (LQ) and uncertainties (expanded U, k=2) for chemical parameters; they were calculated according to standard method NFT90-210 (AFNOR, 2018) and NF ISO 11352 (AFNOR, 2013), respectively. For dissolved organic carbon (DOC), total dissolved nitrogen (NTD) and major ions, uncertainties were derived from results of interlaboratory tests. For trace elements, uncertainties were derived from regular analyses of Certified Reference Material TM-27-4 (lake water, Environment and Climate Change Canada).

	Parameter	Unit	LQ	Uncertainty
Organic matter	DOC	mgC/L	0.2	20%
	NTD	mgN/L	0.2	20%
Major ions	Ca^{2+}	mg/L	4.0	10%
	K^{+}	mg/L	1.0	15%
	Mg^{2+}	mg/L	1.0	13%
	Na^{+}	mg/L	1.0	12%
	NH_4^{+}	mg/L	0.02	14%
	Cl^{-}	mg/L	1.0	7%
	NO_2^{-}	mg/L	0.05	14%
	NO_3^{-}	mg/L	1.0	13%
	PO_4^{3-}	mg/L	0.1	14%
	SO_4^{2-}	mg/L	1.00	9%
	SiO_2	mgSi/L	0.5	12%
Trace elements	Al	µg/L	2.0	20%
	As	µg/L	0.010	20%
	B	µg/L	2.00	25%
	Ba	µg/L	0.01	10%
	Cd	µg/L	0.005	15%
	Co	µg/L	0.005	15%
	Cr	µg/L	0.02	20%
	Cu	µg/L	0.05	15%
	Fe	µg/L	0.10	15%
	Li	µg/L	0.010	20%
	Mn	µg/L	0.05	15%
	Mo	µg/L	0.010	20%
	Ni	µg/L	0.02	20%
	Pb	µg/L	0.01	20%
	Rb	µg/L	0.010	15%*
	Sr	µg/L	0.05	10%
	Ti	µg/L	0.05	25%
	U	µg/L	0.005	20%
	V	µg/L	0.005	20%
	Zn	µg/L	0.50	25%

* uncertainty calculated using coefficient of variation of measured values only (no certified value for this element)

Table A3 – Summary of analytical results for major parameters in source samples. Values are concentrations in mg/L. All analytical results and quality controls are available at: https://entrepot.recherche.data.gouv.fr/dataverse/chypster/)

	BOU (n=5)		VRY (n=5)		VRN (n=5)		REV (n=4)		PNC (n=5)	
Parameter	**Median**	**Range**	**Median**	**Range**	**Median**	**Range**	**Median**	**Range**	**Median**	**Range**
Ca^{2+}	11.1	10.5 - 12.3	6.2	5.5 – 13.0	22.7	21.1 - 40.4	14.6	12.1 - 18.6	15.7	15.3 - 16.9
Cl^-	51.0	49.5 - 56.9	16.0	13.2 - 18.6	6.6	5.8 - 26.7	9.7	7.0 - 16.7	38.0	30.7 - 44.8
K^+	1.0	1.0 – 1.0	1.0	1.0 – 1.0	1.6	1.5 - 2.6	1.0	1.0 – 1.0	2.7	2.2 - 8.3
Mg^{2+}	2.8	2.7 - 3.2	1.9	1.8 - 3.7	3.2	3.0 - 5.7	2.4	2.0 - 3.1	3.0	2.2 - 3.3
Na^+	26.8	25.7 - 34.2	11.3	10.2 - 15.3	8.6	8.1 - 15.4	6.3	5.6 - 7.8	18.6	15.6 - 21.1
SiO_2	20.4	18.4 - 21.1	24.1	20.8 - 25.6	12.7	10.7 - 13.5	11.1	8.3 - 11.9	14.9	11.9 - 16.8
SO_4^{2-}	13.8	12.2 - 15.9	14.1	13.6 – 28.0	18.7	14.9 – 30.0	9.3	6.6 - 13.4	9.5	6.8 - 20.4

	COR (n=5)		PLR (n=4)		RES (n=5)	
Parameter	**Median**	**Range**	**Median**	**Range**	**Median**	**Range**
Ca^{2+}	55.8	25.3 - 64	45.4	28.6 - 96.3	72.8	52.9 - 76.2
Cl^-	29.9	4.6 - 45.7	43.4	25.9 - 74.4	80.8	61.9 - 87.4
K^+	2.9	0.9 - 3.8	3.5	1.9 - 5.2	18.3	12.5 - 21.5
Mg^{2+}	7.5	4.2 - 8.2	3.0	2.0 - 6.9	7.1	4.9 - 7.6
Na^+	26.5	2.3 – 37.0	30.3	17.0 - 44.7	63.2	46.4 - 73.6
SiO_2	32.0	15.5 - 34.8	11.1	6.8 – 12.0	13.3	5.5 - 14.8
SO_4^{2-}	43.7	11.4 - 62.2	41.6	21.1 - 93.2	50.8	33.8 - 58.3

Table A4 – Summary of analytical results for dissolved metals in source samples. Values are concentrations in µg/L. All analytical results and quality controls are available at: https://entrepot.recherche.data.gouv.fr/dataverse/chypster/)

	BOU (n=5)		VRY (n=5)		VRN (n=5)		REV (n=4)		PNC (n=5)	
Parameter	**Median**	**Range**	**Median**	**Range**	**Median**	**Range**	**Median**	**Range**	**Median**	**Range**
Al	126	82.8 - 142	62.5	45.3 - 105	43.2	8.40 - 70.5	75.1	24.3 - 102	29.2	18.9 - 55.9
As	0.49	0.25 - 0.52	0.73	0.58 - 1.11	0.63	0.43 - 0.68	0.53	0.45 - 0.66	4.25	0.93 - 5.28
B	3.00	2.80 - 4.70	3.90	3.70 - 5.00	11.4	8.30 - 18.6	2.80	2.20 - 4.20	2.60	0.20 - 7.30
Ba	20.0	17.9 - 24.4	10.4	9.70 - 18.4	15.4	13.3 - 25.4	13.4	10.4 - 18.7	11.2	9.73 - 20.5
Cd	0.073	0.064 - 0.096	0.023	0.010 - 0.030	0.008	0.005 - 0.021	0.020	0.012 - 0.027	0.009	0.005 - 0.024
Co	0.160	0.144 - 0.173	0.109	0.063 - 0.320	0.125	0.112 - 0.135	0.139	0.115 - 0.213	0.779	0.079 - 1.28
Cr	0.23	0.20 - 0.43	0.37	0.23 - 0.46	0.19	0.15 - 0.29	0.30	0.24 - 0.31	0.26	0.08 - 0.61
Cu	0.42	0.10 - 0.67	0.66	0.10 - 2.75	3.70	3.23 - 4.23	1.77	0.77 - 2.89	0.94	0.74 - 11.3
Li	1.84	1.75 - 2.27	1.42	0.29 - 2.15	0.692	0.622 - 0.753	0.756	0.391 - 1.08	0.759	0.483 - 1.23
Mo	0.045	0.029 - 0.058	0.048	0.029 - 0.057	0.158	0.108 - 0.185	0.0305	0.010 - 0.037	0.304	0.067 - 0.488
Ni	1.13	1.09 - 1.66	1.42	1.14 - 1.67	1.35	0.99 - 2.80	0.99	0.85 - 1.61	0.88	0.44 - 1.08
Pb	0.019	0.005 - 0.032	0.130	0.082 - 0.146	0.013	0.005 - 0.094	0.014	0.005 - 0.024	0.060	0.005 - 0.312
Rb	0.850	0.719 - 1.21	0.724	0.327 - 1.06	0.716	0.598 - 1.19	0.396	0.209 - 0.471	1.30	1.13 - 6.53
Sr	44.1	41.4 - 51.3	40.5	26.5 – 56.0	81.4	75.5 - 138	46.8	27.0 - 68.2	58.9	51.7 - 94.4
Ti	0.52	0.05 - 1.29	1.26	0.27 - 3.94	0.90	0.18 - 2.14	1.80	0.58 - 2.68	0.86	0.75 - 2.73
U	0.298	0.211 - 0.349	0.157	0.005 - 0.303	0.244	0.117 - 0.316	0.148	0.033 - 0.257	0.120	0.079 – 1.00
V	0.289	0.213 - 0.357	0.331	0.229 - 0.403	0.308	0.276 - 0.344	0.297	0.276 - 0.683	0.381	0.258 - 1.02
Zn	1.74	1.33 - 2.16	1.57	0.10 - 1.85	2.63	1.79 - 6.81	2.18	0.93 - 2.76	1.95	1.30 - 73.4

	COR (n=5)		PLR (n4)		RES (n=5)	
Parameter	**Median**	**Range**	**Median**	**Range**	**Median**	**Range**
Al	13.8	7.99 - 97.9	54.3	15.5 - 62.7	17.1	13.9 - 47.5
As	3.05	1.99 - 3.47	2.75	0.68 - 3.34	1.97	1.68 - 2.20
B	17.7	14.9 - 46.5	31.4	15.6 - 36.4	47.9	21.3 - 89.6
Ba	46.4	28.8 - 49.2	29.7	21.0 - 44.5	27.8	25.6 - 34.7
Cd	0.008	0.005 - 0.013	0.027	0.014 - 0.058	0.021	0.014 - 0.107
Co	0.116	0.066 - 0.137	0.276	0.145 - 0.482	0.503	0.122 - 0.579
Cr	0.226	0.033 - 0.65	0.72	0.19 - 1.08	1.06	0.67 - 1.25
Cu	2.00	0.10 - 3.66	8.57	1.07 - 14.3	19.6	9.98 - 24.8
Li	21.1	9.93 - 24.9	1.79	1.15 - 4.22	7.68	1.40 - 8.08
Mo	0.901	0.747 - 1.19	1.20	0.05 - 1.57	1.06	0.749 - 1.39
Ni	0.509	0.020 - 0.594	0.960	0.580 - 1.19	1.56	0.560 - 2.15
Pb	0.124	0.049 - 0.202	0.142	0.039 - 0.588	0.460	0.322 - 0.528
Rb	1.55	0.831 – 2.00	2.53	1.81 - 9.15	14.9	2.22 – 16.0

Sr	181	126 - 219	186	64.1 - 379	247	148 - 272
Ti	0.236	0.126 - 5.67	0.48	0.320 - 3.07	1.45	0.520 - 2.13
U	0.558	0.544 - 0.906	1.69	0.100 - 2.80	1.29	1.12 - 2.73
V	0.919	0.561 - 0.985	1.51	0.408 - 3.53	0.598	0.272 - 1.30
Zn	13.6	4.3 - 13.7	18.6	4.56 - 48.6	36.6	20.4 - 44.2

761

762 **Table A5 – Summary of analytical results for characteristics of dissolved organic matter in source samples. All analytical results**
763 **and quality controls are available at: https://entrepot.recherche.data.gouv.fr/dataverse/chypster/)**

		BOU (n=5)		VRY (n=5)		VRN (n=5)		REV (n=4)		PNC (n=5)	
Parameter	**Unit**	**Median**	**Range**	**Median**	**Range**	**Median**	**Range**	**Median**	**Range**	**Median**	**Range**
DOC	mg/L	2.9	2.7 - 4.6	4.2	3.8 - 4.7	7.5	6.2 - 8.2	8.4	8.4 - 10.1	5.3	4.6 - 10.8
S1	nm^{-1}	0.0160	0.0158 - 0.0163	0.0156	0.0153 - 0.0158	0.0153	0.0151 - 0.0155	0.0151	0.0150 - 0.0155	0.0134	0.0119 - 0.0144
S2	nm^{-1}	0.0196	0.0184 - 0.0203	0.0185	0.0183 - 0.0187	0.0205	0.0199 - 0.0209	0.0213	0.0207 - 0.0220	0.0194	0.0162 - 0.0198
Mn-254	Da	417	323 - 460	542	394 - 593	616	548 - 695	607	596 - 636	569	526 - 703
A0-254	-	4552	2486 - 7349	4772	2165 - 8337	4627	407 - 10478	2404	1501 - 7710	2265	1209 - 4962
A1-254	-	21850	15215 - 34702	47737	46348 - 59736	117263	86123 - 138631	110027	104294 - 117502	67331	50782 - 114518
A2-254	-	48675	38354 - 83965	78227	70245 - 93519	188721	146038 - 204308	216676.5	185118 - 228952	121649	80952 - 176082
A3-254	-	54560	47984 - 128755	65957	54730 - 85950	96041	77790 - 123959	112563	102393 - 121161	62096	53834 - 112852

		COR (n=5)		PLR (n=4)		RES (n=5)	
Parameter	**Unit**	Median	Range	Median	Range	Median	Range
DOC	mg/L	3.5	2.0 - 10.1	6.1	4.4 - 8.4	32.7	22.1 - 42.6
S1	nm^{-1}	0.0123	0.0118 - 0.0145	0.0144	0.0144 - 0.0153	0.0161	0.0104 - 0.0168
S2	nm^{-1}	0.0163	0.0150 - 0.0192	0.0172	0.0167 - 0.0186	0.0127	0.0123 - 0.0128
Mn-254	Da	451	434 - 670	727	621 - 885	424	383 - 579
A0-254	-	4797	144 - 7402	3085	2560 - 9811	6713	4296 - 14343
A1-254	-	33782	18214 - 53643	128469	65410 - 156480	73927	61653 - 100544
A2-254	-	45994	20069 - 65362	137524	86234 - 207418	116338	93322 - 171777
A3-254	-	43102	16900 - 55750	54241	35715 - 114897	129258	85384 - 218065

764

765 **Table A6 – Summary of analytical results for microbial parameters in source samples. Values are concentrations in log10 number**
766 **of copies/100 mL.**

	BOU (n=5)		VRY (n=5)		VRN (n=5)		REV (n=4)		PNC (n=5)	
Parameter	**Median**	**Range**	**Median**	**Range**	**Median**	**Range**	**Median**	**Range**	**Median**	**Range**
HF183	0.0	0.0 – 0.0	0.0	0.0 – 0.0	0.0	0.0 - 1.9	0.0	0.0 – 0.0	0.0	0.0 – 0.0
rum-2-bac	0.0	0.0 – 0.0	0.0	0.0 – 0.0	0.0	0.0 – 0.0	0.0	0.0 – 0.0	0.0	0.0 – 6.0

	COR (n=5)		PLR (n=4)		RES (n=5)	
Parameter	**Median**	**Range**	**Median**	**Range**	**Median**	**Range**
HF183	3.7	3.5 - 6.3	3.5	3.1 - 3.6	7.05	5.7 - 7.5
rum-2-bac	0.0	0.0 – 0.0	0.0	0.0 – 0.0	4.15	3.4 - 4.6

767

768

Table A7 – Mean contributions and standard deviations of estimations obtained for the decomposition of streamwater samples collected during small winter events in March 2019 and March 2023. The values correspond to the relative parts of flow for each time step as a percentage.

		06/03/19 23:15		07/03/19 00:15		07/03/19 01:15		07/03/19 02:15		07/03/19 03:15		07/03/19 04:15		07/03/19 05:15		07/03/19 06:15		07/03/19 07:15		07/03/19 08:15		07/03/19 09:15		07/03/19 10:15	
		Mean	sd	Mean	sd	Mean	sd	Mean	sd	Mean	sd	Mean	sd	Mean	sd	Mean	sd	Mean	sd	Mean	sd	Mean	sd	Mean	sd
06/03/2019 - Mercier	FOR_1	17	12	34	7	25	7	30	8	32	8	31	8	33	8	33	8	34	8	35	8	36	8	32	9
	FOR_2	5	5	4	4	6	8	5	6	4	5	4	5	5	6	5	7	4	6	4	5	4	5	3	3
	GRA	31	11	20	5	26	8	27	7	15	6	12	6	16	6	17	7	19	7	19	7	19	7	11	5
	AGR	32	21	7	6	8	8	7	8	8	9	11	9	11	8	9	7	8	7	7	7	6	7	6	8
	URB	0	0	5	6	3	4	5	6	5	7	5	7	5	6	5	6	6	7	6	8	6	8	7	10
	SEW	16	4	15	3	11	2	13	3	19	3	19	3	17	3	18	3	18	3	19	4	18	4	21	4
	SUR	0	0	15	3	21	5	13	4	16	5	17	5	14	4	13	4	12	4	10	4	11	4	20	5

		13/03/23 18:37		13/03/23 19:07		13/03/23 19:37		13/03/23 20:07		13/03/23 20:37		13/03/23 21:07		13/03/23 21:37		13/03/23 22:07		13/03/23 22:37		13/03/23 23:07		13/03/23 23:37		14/03/23 00:07	
		Mean	sd	Mean	sd	Mean	sd	Mean	sd	Mean	sd	Mean	sd	Mean	sd	Mean	sd	Mean	sd	Mean	sd	Mean	sd	Mean	sd
13/03/2023 - Mercier	FOR_1	13	11	6	5	14	12	5	5	6	6	9	8	8	7	7	6	4	4	4	3	5	5	6	6
	FOR_2	3	3	14	6	12	9	43	19	36	18	27	15	23	13	23	13	25	14	26	15	26	15	22	13
	GRA	35	23	6	6	8	8	9	6	8	6	8	9	7	12	6	13	6	13	8	13	9	11	11	10
	AGR	23	22	8	4	8	8	6	9	6	8	9	7	13	6	16	5	15	5	15	7	13	8	12	9
	URB	0	0	52	7	48	11	19	5	19	5	31	7	23	8	18	7	17	7	18	7	22	7	27	8
	SEW	26	5	7	3	5	3	2	1	2	1	5	2	11	4	14	4	15	4	14	4	15	4	15	4
	SUR	0	0	7	2	5	3	15	8	23	8	10	6	14	7	18	7	18	7	16	7	9	6	8	5

		13/03/23 18:30		13/03/23 20:45		13/03/23 22:07		13/03/23 22:37		13/03/23 23:15		13/03/23 23:30		13/03/23 23:45		14/03/23 00:00		14/03/23 00:15	
		Mean	sd	Mean	sd	Mean	sd	Mean	sd	Mean	sd	Mean	sd	Mean	sd	Mean	sd	Mean	sd
13/03/2023 - Ratier	FOR_1	14	10	3	3	3	4	3	3	2	2	2	2	2	2	3	3	4	4
	FOR_2	7	6	2	2	2	2	2	2	1	2	1	2	1	2	2	3	2	3
	GRA	13	11	21	6	21	9	18	7	20	8	19	8	21	8	22	8	22	8
	AGR	9	8	7	4	6	6	9	7	5	5	5	5	6	6	10	8	10	8
	AQU	44	11	1	1	1	1	1	1	1	1	1	1	1	1	1	1	1	1
	URB	0	0	28	6	44	12	29	9	43	10	47	11	39	10	35	10	36	10
	SEW	13	7	4	2	6	4	6	3	5	3	5	3	6	3	6	3	8	3
	SUR	0	0	35	4	18	5	32	4	22	5	19	5	23	5	20	5	17	5

Table A8 – Mean contributions and standard deviations of estimations obtained for the decomposition of streamwater samples collected during summer storm events in June 2022 and September 2022. The values correspond to the relative parts of flow for each time step as a percentage.

		22/06/22 15:07		22/06/22 15:37		22/06/22 16:07		22/06/22 16:37		22/06/22 17:07		22/06/22 17:37		22/06/22 18:07		22/06/22 18:37		22/06/22 19:07		22/06/22 19:37		22/06/22 20:07	
		Mean	sd	Mean	sd	Mean	sd	Mean	sd	Mean	sd	Mean	sd	Mean	sd	Mean	sd	Mean	sd	Mean	sd	Mean	sd
22/06/2022 - Ratier	FOR_1	0	0	0	1	1	1	0	1	0	1	0	1	0	1	0	1	0	1	0	1	0	1
	FOR_2	1	1	1	2	3	5	2	3	1	2	1	2	1	2	1	2	1	2	2	2	2	2
	GRA	5	4	6	7	14	10	11	10	6	6	11	10	12	11	8	7	6	6	7	7	7	7
	AGR	1	2	1	2	3	4	2	3	1	2	1	2	2	3	2	3	3	7	3	5	3	5
	AQU	16	21	3	4	6	7	3	4	2	2	2	3	2	3	2	3	3	4	3	3	3	3
	URB	48	34	34	26	23	17	21	17	19	15	17	14	17	14	17	13	26	19	23	18	24	18
	SEW	8	8	6	5	6	4	5	4	4	3	3	3	4	3	5	3	12	7	10	6	10	6
	SUR	20	9	48	23	44	15	56	17	66	15	64	17	61	16	65	13	48	15	52	15	51	17

		14/09/22 17:20		14/09/22 17:35		14/09/22 17:55		14/09/22 18:15		14/09/22 18:35		14/09/22 18:55		14/09/22 19:15		14/09/22 19:35		14/09/22 19:55		14/09/22 20:15	
		Mean	sd	Mean	sd	Mean	sd	Mean	sd	Mean	sd	Mean	sd	Mean	sd	Mean	sd	Mean	sd	Mean	sd
09/09/2022 - Mercier	FOR_1	0	0	0	0	0	0	0	0	0	1	0	1	0	1	0	1	1	1	1	1
	FOR_2	1	1	1	1	1	2	1	2	1	2	1	3	2	3	2	3	2	3	2	3
	GRA	31	22	39	28	34	24	34	24	38	27	36	25	35	24	34	23	33	22	34	23
	AGR	1	5	1	4	1	5	1	5	1	6	1	7	2	7	2	8	2	8	3	8
	URB	33	1	17	1	22	1	22	1	19	2	22	2	25	2	27	3	30	3	29	4
	SEW	1	0	0	0	0	0	0	1	0	1	1	1	1	1	1	1	1	1	1	1
	SUR	32	22	42	28	42	24	41	23	40	24	38	21	35	20	34	19	32	17	31	18

		14/09/22 16:35		14/09/22 16:55		14/09/22 17:15		14/09/22 17:35		14/09/22 17:55		14/09/22 18:15		14/09/22 18:35		14/09/22 18:55		14/09/22 19:15		14/09/22 19:35		14/09/22 19:55		14/09/22 20:15	
		Mean	sd	Mean	sd	Mean	sd	Mean	sd	Mean	sd	Mean	sd	Mean	sd	Mean	sd	Mean	sd	Mean	sd	Mean	sd	Mean	sd
09/09/2022 - Ratier	FOR_1	3	3	3	4	0	0	0	0	0	0	0	0	0	0	0	1	0	1	0	1	1	1	1	1
	FOR_2	4	3	4	4	1	1	0	1	0	1	0	1	1	1	1	1	1	1	1	2	1	2	1	2
	GRA	3	3	4	4	26	4	35	5	41	5	46	5	45	5	44	5	43	5	41	6	38	6	38	7
	AGR	5	4	6	6	2	2	1	1	1	1	1	1	1	1	1	2	1	2	2	2	2	3	3	4
	AQU	72	5	70	5	40	3	4	2	4	2	3	1	4	2	5	2	7	2	10	2	12	2	15	3
	URB	0	0	0	0	2	2	1	2	1	1	1	1	1	1	1	1	1	2	2	2	2	3	3	4
	SEW	13	6	14	6	9	2	7	1	4	1	2	1	2	1	2	1	2	1	3	1	3	1	4	2
	SUR	0	0	0	0	20	3	51	4	49	4	47	4	46	4	46	4	44	4	41	5	40	5	35	5.66

Table A9 – Mean contributions and standard deviations of estimations obtained for the decomposition of streamwater samples collected during major events in May 2021 and October 2021. The values correspond to the relative parts of flow for each time step as a percentage.

		10/05/21 09:45		10/05/21 10:45		10/05/21 11:45		10/05/21 12:45		10/05/21 13:45		10/05/21 14:45		10/05/21 15:45		10/05/21 16:45		10/05/21 17:45		10/05/21 18:45		10/05/21 19:45		10/05/21 20:45	
		Mean	sd	Mean	sd	Mean	sd	Mean	sd	Mean	sd	Mean	sd	Mean	sd	Mean	sd	Mean	sd	Mean	sd	Mean	sd	Mean	sd
10/05/2021 - Mercier	FOR_1	1	1	2	3	1	2	1	2	1	1	1	1	1	1	1	1	1	1	1	2	1	1	1	1
	FOR_2	2	3	2	3	3	4	3	4	2	3	2	3	2	3	2	3	2	3	3	4	3	4	3	4
	GRA	10	4	7	5	9	6	9	6	8	6	10	7	11	7	14	7	12	7	17	8	19	9	19	9
	AGR	66	11	67	15	63	16	62	17	66	17	64	16	64	16	59	15	62	15	59	14	57	14	59	14
	URB	2	2	2	2	2	2	2	2	2	2	2	2	2	2	2	3	2	3	2	3	2	3	2	2
	SEW	6	3	7	4	5	4	5	4	4	4	4	4	5	4	7	4	6	4	7	4	8	4	7	4
	SUR	13	9	12	11	17	12	18	13	17	13	16	12	15	12	14	11	14	11	11	9	10	8	9	7

		10/05/21 10:15		10/05/21 11:15		10/05/21 12:15		10/05/21 13:15		10/05/21 14:15		10/05/21 15:15		10/05/21 16:15		10/05/21 17:15		10/05/21 18:15		10/05/21 19:15		10/05/21 20:15		10/05/21 21:15	
		Mean	sd	Mean	sd	Mean	sd	Mean	sd	Mean	sd	Mean	sd	Mean	sd	Mean	sd	Mean	sd	Mean	sd	Mean	sd	Mean	sd
10/05/2021 - Ratier	FOR_1	0	0	1	1	1	1	1	1	0	1	0	1	0	1	0	1	0	1	0	1	0	1	1	1
	FOR_2	1	1	1	2	1	2	1	1	1	1	1	1	1	1	1	1	1	1	1	1	1	2	1	2
	GRA	10	4	11	6	11	6	10	6	10	6	11	7	9	6	10	6	11	7	13	8	13	8	15	9
	AGR	21	4	21	6	17	6	22	6	22	6	26	7	31	7	33	7	35	7	39	8	41	9	45	11
	AQU	0	0	0	0	0	1	0	1	0	0	0	0	0	0	0	0	0	0	0	0	0	0	0	0
	URB	12	5	11	5	19	7	18	7	15	7	15	7	15	7	15	7	15	7	14	7	13	7	13	7
	SEW	4	2	4	2	5	3	5	3	5	3	5	3	4	3	5	3	4	3	5	3	5	3	6	4
	SUR	51	3	52	3	45	4	43	4	47	4	43	4	40	5	37	5	33	5	28	5	25	5	19	5

		03/10/21 14:37		03/10/21 16:07		03/10/21 17:37		03/10/21 19:07		03/10/21 20:37		03/10/21 22:07		03/10/21 23:37		04/10/21 01:07		04/10/21 02:37		04/10/21 04:07		04/10/21 05:37		04/10/21 07:07	
		Mean	sd	Mean	sd	Mean	sd	Mean	sd	Mean	sd	Mean	sd	Mean	sd	Mean	sd	Mean	sd	Mean	sd	Mean	sd	Mean	sd
03/10/2021 - Mercier	FOR_1	1	1	0	0	0	1	0	1	0	1	1	1	0	1	1	1	1	1	1	1	1	1	1	1
	FOR_2	1	1	1	1	1	2	1	2	1	2	1	2	1	2	2	2	2	3	2	3	2	2	2	2
	GRA	26	6	16	9	13	6	15	7	17	7	21	8	24	8	30	8	30	8	33	8	34	8	32	8
	AGR	40	6	33	8	47	8	47	9	43	9	45	9	44	9	39	9	38	9	36	9	33	9	33	9
	URB	4	3	2	2	2	2	3	3	3	3	3	3	3	3	4	4	6	5	6	5	6	6	7	6
	SEW	9	2	2	2	2	1	5	2	6	2	5	2	6	3	10	3	13	3	13	3	14	3	15	3
	SUR	20	4	47	6	35	5	29	6	28	6	24	6	20	6	15	5	11	4	9	4	10	4	11	4

		03/10/21 14:37		03/10/21 16:07		03/10/21 17:37		03/10/21 19:07		03/10/21 20:37		03/10/21 22:07		03/10/21 23:37		04/10/21 01:07		04/10/21 02:37		04/10/21 04:07		04/10/21 05:37		04/10/21 07:07	
		Mean	sd	Mean	sd	Mean	sd	Mean	sd	Mean	sd	Mean	sd	Mean	sd	Mean	sd	Mean	sd	Mean	sd	Mean	sd	Mean	sd
03/10/2021 - Ratier	FOR_1	1	1	0	1	1	1	1	1	1	1	1	1	1	1	1	1	1	1	1	1	1	2	1	2
	FOR_2	2	2	1	2	1	2	2	3	2	3	2	3	2	3	3	4	3	4	2	4	3	4	3	4
	GRA	10	5	9	7	13	10	13	9	11	8	13	9	12	8	12	8	14	9	12	9	16	10	14	10
	AGR	13	9	10	9	14	12	18	14	19	15	20	15	22	16	24	17	24	18	23	20	22	17	22	17
	AQU	2	6	0	1	1	1	1	1	1	1	1	1	1	1	1	1	1	2	1	2	1	2	1	2
	URB	52	11	22	8	29	11	26	11	27	11	28	12	31	12	34	12	35	12	44	14	40	12	43	11
	SEW	5	7	1	1	1	1	1	2	2	2	2	2	2	2	3	3	3	4	3	5	4	4	5	5
	SUR	16	4	56	6	40	8	39	7	38	7	34	7	30	7	24	7	19	7	14	7	13	6	11	6

783
784

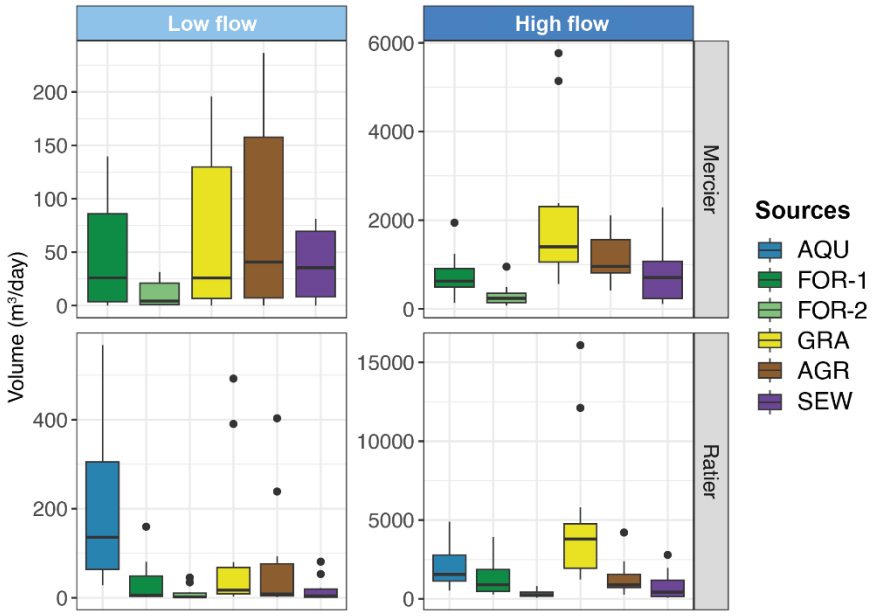

Figure A1 – Daily volume contributions in m^3 estimated for dry weather streamwater samples by the application of a biogeochemical decomposition using a Bayesian mixing model for the Mercier and Ratier catchments. Contributions in terms of volume were calculated based on the relative contributions for each source and the total flow for each sampled day in m^3. Boxplots represent the median contribution, interquartile range (1st and 3rd quartiles), minimum and maximum values. Low flow samples correspond to a mean daily discharge lower than 20 L/s and high flow samples to a mean daily discharge higher than 20 L/s.

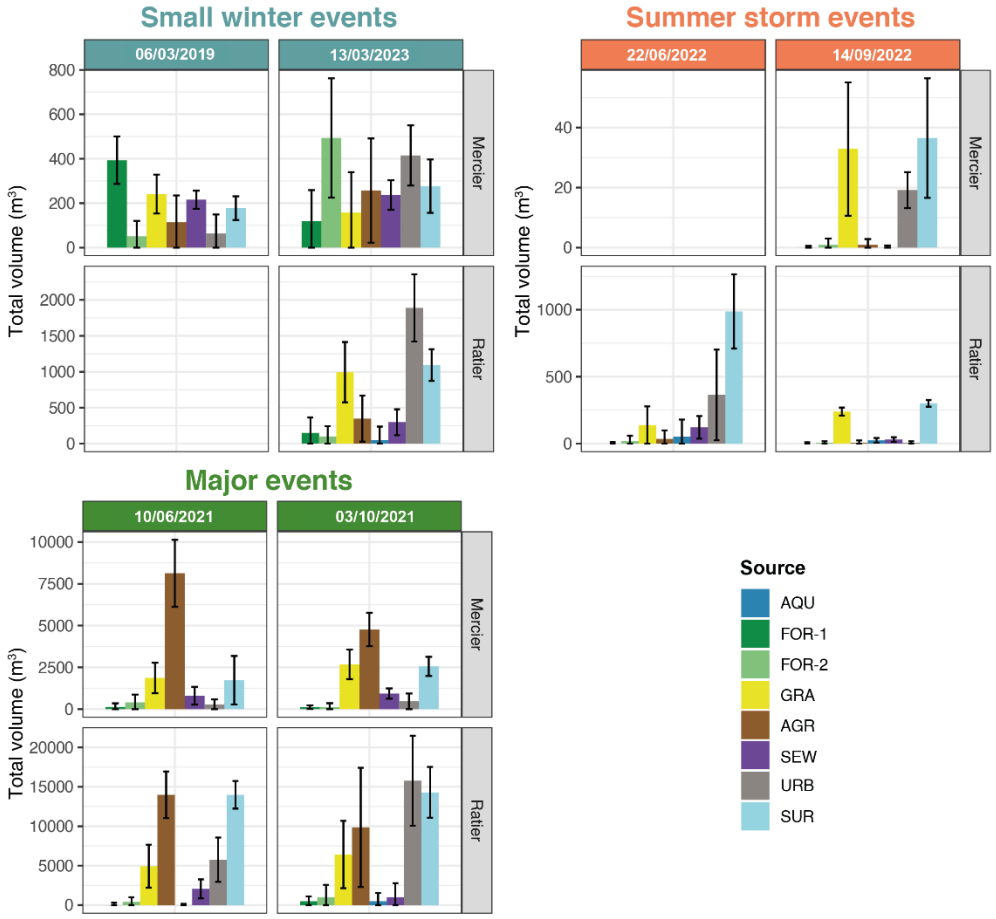

Figure A2 – Total volume contributions to the hydrological events sampled between March 2019 and March 2023 at the outlets of the Mercier and Ratier catchments. Contributions in terms of volume were calculated based on the relative contributions from each source and the total flow in m^3. The contributions correspond to the mean of the results obtained for each sample decomposition by the Bayesian mixing model. The error bars correspond to the mean of the standard deviation calculated from the sum of the squares of the deviation. The events of 6 March 2019 at the Ratier station and 22 June 2022 at the Mercier station were not collected.

Data availability

Hydro-meteorological data and biogeochemical data at the catchment outlets during dry weather is available online at https://bdoh.irstea.fr/YZERON/station/V3015810 and https://bdoh.irstea.fr/YZERON/station/V301502401, respectively for the Mercier and the Ratier station (https://doi.org/10.57745/VVQ2X9; https://doi.org/10.17180/obs.yzeron). Metadata relative to the sampling of sources and of the catchment outlets are detailed at: https://doi.org/10.57745/K3S9YV. Biogeochemical data of the sources and at the catchment outlets during hydrological events is available at https://doi.org/10.57745/HQPIFQ for major parameters and dissolved metals, and at https://doi.org/10.57745/IYJ2VE for characteristics of DOM.

Author contributions

OG: Writing – original draft, Visualization, Methodology, Investigation, Formal analysis, Conceptualization. **FB**: Writing – review & editing, Investigation, Methodology, Conceptualization. **MM**: Writing – review & editing, Investigation, Methodology, Conceptualization. **BC**: Writing – review & editing, Investigation, Methodology. **NR**: Writing – review & editing, Investigation, Methodology. **PD**: Writing – review & editing, Investigation, Methodology. **ADL**: Writing – review & editing, Investigation, Methodology. **MC**: Writing – review & editing, Investigation, Methodology, Conceptualization, Funding acquisition, Project administration.

Declaration of competing interest

The authors declare that they have no known competing financial interests or personal relationships that could have appeared to influence the work reported in this paper.

Acknowledgements

Authors thanks Corinne Brosse-Quilgars, Lysiane Dherret, Loïc Richard, Aymeric Dabrin, Amandine Daval and Christelle Margoum of the Aquatic Chemistry Laboratory team of RiverLy (INRAE), and Laurence Marjolet and B. Youenou of UMR Ecologie Microbienne (VetAgro Sup) for the analysis of the samples, as well as M. Lagouy (INRAE, RiverLy) for field sampling. We also thank the OTHU (Field Observatory in Urban Hydrology) and OZCAR (Critical Zone Observatories: Research and Application) observatories for data provision. This work was carried out in the frame of a PhD, which was partly funded by EUR H2O Lyon, and in the frame of the CHYPSTER research project partly funded by the French National Research Agency (ANR-21-CE34-0013-01) and the IDESOC project granted by the ZABR – Rhone Basin LTSER within the Water Agency RMC – RB LTSER funding agreement.

References

AFNOR: Standard method NF ISO 11352. Water Quality - Estimation of measurement uncertainty based on validation and quality control data., 2013.

AFNOR: Standard method NF T90-210. Water quality - Protocol for the intial method performance assesment in a laboratory., 2018.

Aussel, H., Bâcle, C. L., and Dornier, G.: Le traitement des eaux usées, INRS, 2004.

Barthold, F. K., Wu, J., Vaché, K. B., Schneider, K., Frede, H.-G., and Breuer, L.: Identification of geographic runoff sources in a data sparse region: hydrological processes and the limitations of tracer-based approaches, Hydrological Processes, 24, 2313–2327, https://doi.org/10.1002/hyp.7678, 2010.

Becouze-Lareure, C.: Caractérisation et estimation des flux de substances prioritaires dans les rejets urbains par temps de pluie sur deux bassins versants expérimentaux, phd, Thèse de doctorat, 2010.

Begum, M. S., Park, H.-Y., Shin, H.-S., Lee, B.-J., and Hur, J.: Separately tracking the sources of hydrophobic and hydrophilic dissolved organic matter during a storm event in an agricultural watershed, Science of The Total Environment, 873, 162347, https://doi.org/10.1016/j.scitotenv.2023.162347, 2023.

Benjamin, M. M.: Water Chemistry: Second Edition, Waveland Press, 2014.

Bétemps, M.: Diagnostic de l'occupation du sol et de l'utilisation des produits chimiques sur le bassin versant de l'Yzeron (Rhône) : utilisation combinée d'enquêtes et de données cartographiques pour identifier les sources de contaminants et leur localisation., master, Mémoire de Master, Université Grenobles Alpes, Laboratoire IGE Cermosem, 2021.

Beven, K.: Rainfall-runoff modelling : the primer, second edition, John Wiley & Sons, Ltd, 2012.

Birkel, C. and Soulsby, C.: Advancing tracer-aided rainfall-runoff modelling: A review of progress, problems and unrealised potential, Hydrological Processes, 29, 5227–5240, https://doi.org/10.1002/hyp.10594, 2015.

Birkinshaw, S. J., O'Donnell, G., Glenis, V., and Kilsby, C.: Improved hydrological modelling of urban catchments using runoff coefficients, Journal of Hydrology, 594, 125884, https://doi.org/10.1016/j.jhydrol.2020.125884, 2021.

Bomboï, M. T. and Hernandez, A.: Hydrocarbons in urban runoff : their contribution to thewastewaters., Water Research, 25, 557–565, 1991.

Bouchali, R., Mandon, C., Danty - Berger, E., Géloën, A., Marjolet, L., Youenou, B., Pozzi, A. C. M., Vareilles, S., Galia, W., Kouyi, G. L., Toussaint, J.-Y., and Cournoyer, B.: Runoff microbiome quality assessment of a city center rainwater harvesting zone shows a differentiation of pathogen loads according to human mobility patterns, International Journal of Hygiene and Environmental Health, 260, 114391, https://doi.org/10.1016/j.ijheh.2024.114391, 2024.

Boukra, A., Masson, M., Brosse, C., Sourzac, M., Parlanti, E., and Miège, C.: Sampling terrigenous diffuse sources in watercourse: Influence of land use and hydrological conditions on dissolved organic matter characteristics, Science of The Total Environment, 872, 162104, https://doi.org/10.1016/j.scitotenv.2023.162104, 2023.

Braud, I., Branger, F., Chancibault, K., Jacqueminet, C., Breil, P., Chocat, B., Debionne, S., Dodane, C., Honegger, A., Joliveau, T., Kermadi, S., Leblois, E., Lipeme Kouyi, G., Michel, K., Mosini, M. L., Renard, F., Rodriguez, F., Sarrazin, B.,

Schmitt, L., Andrieu, H., Bocher, E., Comby, J., and Viallet, P.: Assessing the vulnerability of PeriUrban rivers. Rapport scientifique final du projet AVuPUR (ANR-07-VULN-01), IRSTEA, 2011.

Braud, I., Breil, P., and Lagouy, M.: Surveillance, prévision des crues et inondations dans le bassin de l'Yzeron : Etude de définition d'un système d'interprétation des relations entre la saturation des sols, les précipitations et les débits, Irstea, 2018.

Bruijnzeel, L. A.: Hydrological functions of tropical forests: not seeing the soil for the trees?, Agriculture, Ecosystems & Environment, 104, 185–228, https://doi.org/10.1016/j.agee.2004.01.015, 2004.

Burns, D. A., McDonnell, J., Hooper, R. P., Peters, N. E., Freer, J. E., Kendall, C., and Beven, K.: Quantifying contributions to storm runoff through end-member mixing analysis and hydrologic measurements at the Panola Mountain research watershed (Georgia, USA), Hydrological Processes, 15, 1903–1924, https://doi.org/10.1002/hyp.246, 2001.

Cabral Nascimento, R., Jamil Maia, A., Jacques Agra Bezerra da Silva, Y., Farias Amorim, F., Williams Araújo do Nascimento, C., Tiecher, T., Evrard, O., Collins, A. L., Miranda Biondi, C., and Jacques Agra Bezerra da Silva, Y.: Sediment source apportionment using geochemical composite signatures in a large and polluted river system with a semiarid-coastal interface, Brazil, CATENA, 220, 106710, https://doi.org/10.1016/j.catena.2022.106710, 2023.

Charters, F. J., Cochrane, T. A., and O'Sullivan, A. D.: Untreated runoff quality from roof and road surfaces in a low intensity rainfall climate, Science of The Total Environment, 550, 265–272, https://doi.org/10.1016/j.scitotenv.2016.01.093, 2016.

Chocat, B., Krebs, P., Marsalek, J., Rauch, W., and Schilling, W.: Urban drainage redefined: from stormwater removal to integrated management, Water Science and Technology, 43, 61–68, https://doi.org/10.2166/wst.2001.0251, 2001.

Christophersen, N. and Hooper, R. P.: Multivariate analysis of stream water chemical data: The use of principal components analysis for the end-member mixing problem, Water Resources Research, 28, 99–107, https://doi.org/10.1029/91WR02518, 1992.

Christophersen, N., Neal, C., Hooper, R., Vogt, R., and Andersen, S.: Modeling streamwater chemistry as a mixture of soil water end-members - a step towards second generation acidification models, Journal of Hydrology, 116, 307–320, https://doi.org/10.1016/0022-1694(90)90130-P, 1990.

Colin, Y., Bouchali, R., Marjolet, L., Marti, R., Vautrin, F., Voisin, J., Bourgeois, E., Rodriguez-Nava, V., Blaha, D., Winiarski, T., Mermillod-Blondin, F., and Cournoyer, B.: Coalescence of bacterial groups originating from urban runoffs and artificial infiltration systems among aquifer microbiomes, Hydrol. Earth Syst. Sci., 24, 4257–4273, https://doi.org/10.5194/hess-24-4257-2020, 2020.

Collins, A. L., Walling, D. E., and Leeks, G. J. L.: Use of the geochemical record preserved in floodplain deposits to reconstruct recent changes in river basin sediment sources, Geomorphology, 19, 151–167, https://doi.org/10.1016/S0169-555X(96)00044-X, 1997.

Collins, A. L., Pulley, S., Foster, I. D. L., Gellis, A., Porto, P., and Horowitz, A. J.: Sediment source fingerprinting as an aid to catchment management: A review of the current state of knowledge and a methodological decision-tree for end-users, Journal of Environmental Management, 194, 86–108, https://doi.org/10.1016/j.jenvman.2016.09.075, 2017.

Cooper, D. M., Jenkins, A., Skeffington, R., and Gannon, B.: Catchment-scale simulation of stream water chemistry by spatial mixing: Theory and application, Journal of Hydrology, 233, 121–137, https://doi.org/10.1016/S0022-1694(00)00230-4, 2000.

Coquery, M., Pomies, M., Martin Ruel, S., Budzinski, H., Miege, C., Esperanza, M., Soulier, C., and Choubert, J. M.: Mesurer les micropolluants dans les eaux usées brutes et traitées. Protocoles et résultats pour l'analyse des concentrations et des flux, Techniques Sciences Méthodes, 1–2, 25–43, 2011.

Cristiano, E., ten Veldhuis, M.-C., and van de Giesen, N.: Spatial and temporal variability of rainfall and their effects on hydrological response in urban areas – a review, Hydrology and Earth System Sciences, 21, 3859–3878, https://doi.org/10.5194/hess-21-3859-2017, 2017.

David, L., Elmi, S., and Féraud, J.: Carte géologique de la france au 1/50 000 - lyon. Feuille XXX-31, BRGM, Service Géologique National, 41, 1979.

Deletic, A. and Orr, D. W.: Pollution buildup on road surfaces, Journal of Environmental Engineering, 131, 49–59, https://doi.org/10.1061/(ASCE)0733-9372(2005)131:1(49), 2005.

Delfour, J., Dufour, E., Feybesse, J. I., Johan, V., Kerrien, Y., Lardeaux, J. M., Lemière, B., Mouterde, R., and Tegyey, M.: Notice explicative, carte géol. France (1/50000), feuille tarare (697), Orléans: Bureau de recherches géologiques et minières, 120, 1989.

Dubois, V., Falipou, E., and Boutin, C.: Quantification and qualification of the urban domestic pollution discharged per household and per resident, Water Sci Technol, 85, 1484–1499, https://doi.org/10.2166/wst.2022.064, 2022.

Dunn, O. J.: Multiple comparisons using rank sums, Technometrics, 6, 241–252, https://doi.org/10.2307/1266041, 1964.

El Azzi, D., Probst, J. L., Teisserenc, R., Merlina, G., Baqué, D., Julien, F., Payre-Suc, V., and Guiresse, M.: Trace element and pesticide dynamics during a flood event in the save agricultural watershed: soil-river transfer pathways and controlling factors, Water, Air, and Soil Pollution, 227, https://doi.org/10.1007/s11270-016-3144-0, 2016.

Eme, C. and Boutin, C.: Composition des eaux usées domestiques par source d'émission à l'échelle de l'habitation. Etude bibliographique, irstea, 2015.

Emmanuel, I., Andrieu, H., Flahaut, B., and Furusho, C.: Influence of rainfall spatial variability on rainfall runoff modelling: case study on a peri-urban catchment, 2012.

Fines, R. W., Stone, M., Webster, K. L., Leach, J. A., Buttle, J. M., Emelko, M. B., and Collins, A. L.: Evaluation of Legacy Forest Harvesting Impacts on Dominant Stream Water Sources and Implications for Water Quality Using End Member Mixing Analysis, WATER, 15, https://doi.org/10.3390/w15152825, 2023.

Froger, C., Quantin, C., Bordier, L., Monvoisin, G., Evrard, O., and Ayrault, S.: Quantification of spatial and temporal variations in trace element fluxes originating from urban areas at the catchment scale, Journal of Soils and Sediments, 20, 4055–4069, https://doi.org/10.1007/s11368-020-02766-1, 2020.

Fröhlich, H. L., Breuer, L., Vaché, K. B., and Frede, H.-G.: Inferring the effect of catchment complexity on mesoscale hydrologic response, Water Resources Research, 44, https://doi.org/10.1029/2007WR006207, 2008a.

Fröhlich, H. L., Breuer, L., Frede, H.-G., Huisman, J. A., and Vaché, K. B.: Water source characterization through spatiotemporal patterns of major, minor and trace element stream concentrations in a complex, mesoscale German catchment, Hydrological Processes, 22, 2028–2043, https://doi.org/10.1002/hyp.6804, 2008b.

Giri, S. and Qiu, Z.: Understanding the relationship of land uses and water quality in Twenty First Century: A review, Journal of Environmental Management, 173, 41–48, https://doi.org/10.1016/j.jenvman.2016.02.029, 2016.

Gnouma, R.: Aide à la calibration d'un modèle hydrologique distribué au moyen d'une analyse des processus hydrologiques : application au bassin versant de l'Yzeron, phd, Thèse de doctorat, INSA Lyon, 2006.

Gonzales, A. L., Nonner, J., Heijkers, J., and Uhlenbrook, S.: Comparison of different base flow separation methods in a lowland catchment, Hydrology and Earth System Sciences, 13, 2055–2068, https://doi.org/10.5194/hess-13-2055-2009, 2009.

Goutaland, D.: Programme ANR AVuPUR - Prospection géophysique par panneau éléctrique de trois parcelles d'un sous-bassin versant de l'Yzeron, CETE de Lyon, 2009.

Grandjouan, O.: Apports de la biogéochimie pour l'évaluation d'un modèle hydrologique distribué en milieu péri-urbain, phd, Thèse de doctorat, INRAE, 2024.

Grandjouan, O., Branger, F., Masson, M., Cournoyer, B., and Coquery, M.: Identification and estimation of hydrological contributions in a mixed land-use catchment based on a simple biogeochemical and hydro-meteorological dataset, Hydrological Processes, 37, e15035, https://doi.org/10.1002/hyp.15035, 2023.

Helms, J. R., Stubbins, A., Ritchie, J. D., Minor, E. C., Kieber, D. J., and Mopper, K.: Absorption spectral slopes and slope ratios as indicators of molecular weight, source, and photobleaching of chromophoric dissolved organic matter, Limnology and Oceanography, 53, 955–969, https://doi.org/10.4319/lo.2008.53.3.0955, 2008.

Iorgulescu, I., Beven, K. J., and Musy, A.: Data-based modelling of runoff and chemical tracer concentrations in the Haute-Mentue research catchment (Switzerland), Hydrological Processes, 19, 2557–2573, https://doi.org/10.1002/hyp.5731, 2005.

Jacqueminet, C., Kermadi, S., Michel, K., Béal, D., Gagnage, M., Branger, F., Jankowfsky, S., and Braud, I.: Land cover mapping using aerial and VHR satellite images for distributed hydrological modelling of periurban catchments: Application to the Yzeron catchment (Lyon, France), Journal of Hydrology, 485, 68–83, https://doi.org/10.1016/j.jhydrol.2013.01.028, 2013.

James, R., Amasi, A. I., Wynants, M., Nobert, J., Mtei, K. M., and Njau, K.: Tracing the dominant sources of sediment flowing towards Lake Victoria using geochemical tracers and a Bayesian mixing model, J Soils Sediments, 23, 1568–1580, https://doi.org/10.1007/s11368-023-03440-y, 2023.

Jankowfsky, S.: Understanding and modelling of hydrological processes in small peri-urban catchments using an object-oriented and modular distributed approach Application to the Chaudanne and Mercier sub-catchments (Yzeron catchment, France), Theses, Thèse de doctorat, spécialité Océan, Atmosphère, Hydrologie, Ecole Doctorale Terre Univers Environnement, Université de Grenoble, 2011.

Kaown, D., Koh, D.-C., Mayer, B., Mahlknecht, J., Ju, Y., Rhee, S.-K., Kim, J.-H., Park, D. K., Park, I., Lee, H.-L., Yoon, Y.-Y., and Lee, K.-K.: Estimation of nutrient sources and fate in groundwater near a large weir-regulated river using multiple isotopes and microbial signatures, Journal of Hazardous Materials, 446, 130703, https://doi.org/10.1016/j.jhazmat.2022.130703, 2023.

Kermadi, S., Braud, I., Jacqueminet, C., Branger, F., Renard, F., and Michel, K.: Quels liens entre climatologie, occupation des sols et inondations dans le bassin versant de l'Yzeron (ouest Lyonnais) ? Apport de l'analyse conjointe de données hydroclimatiques et d'images satellitaires très haute résolution, Climatologie, 9, 83, 2012.

Klages, M. G. and Hsieh, Y. P.: Suspended Solids Carried by the Gallatin River of Southwestern Montana: II. Using Mineralogy for Inferring Sources, Journal of Environmental Quality, 4, 68–73, https://doi.org/10.2134/jeq1975.00472425000400010016x, 1975.

Kruskal, W. H. and Wallis, W. A.: Use of ranks in one-criterion variance analysis, Journal of the American Statistical Association, 47, 583–621, https://doi.org/10.2307/2280779, 1952.

Kuhlemann, L.-M., Tetzlaff, D., and Soulsby, C.: Spatio-temporal variations in stable isotopes in peri-urban catchments: A preliminary assessment of potential and challenges in assessing streamflow sources, Journal of Hydrology, 600, 126685, https://doi.org/10.1016/j.jhydrol.2021.126685, 2021.

Kumar, N., Ganguly, A., Biswal, K., Keesari, T., Pandey, A., and Deshpande, R. D.: Relative contribution from different water sources to supraglacial runoff in western Himalaya, Journal of Hydrology, 635, 131137, https://doi.org/10.1016/j.jhydrol.2024.131137, 2024.

Labbas, M.: Modélisation hydrologique de bassins versants périurbains et influence de l'occupation du sol et de la gestion des eaux pluviales. Application au bassin de l'Yzeron (130 km2), phd, Thèse de doctorat, Université Grenoble Alpes, 2014.

Lachassagne, P., Dewandel, B., and Wyns, R.: Review: Hydrogeology of weathered crystalline/hard-rock aquifers—guidelines for the operational survey and management of their groundwater resources, Hydrogeol J, 29, 2561–2594, https://doi.org/10.1007/s10040-021-02339-7, 2021.

Ladouche, B., Probst, A., Viville, D., Idir, S., Baqué, D., Loubet, M., Probst, J.-L., and Bariac, T.: Hydrograph separation using isotopic, chemical and hydrological approaches (Strengbach catchment, France), Journal of Hydrology, 242, 255–274, https://doi.org/10.1016/S0022-1694(00)00391-7, 2001.

Lafont, M., Vivier, A., Nogueira, S., Namour, P., and Breil, P.: Surface and hyporheic oligochaete assemblages in a french suburban stream, Hydrobiologia, 564, 183–193, https://doi.org/10.1007/s10750-005-1718-8, 2006.

Lagouy, M., Branger, F., and Breil, P.: Rainfall monitoring on the Yzeron catchment since 1997, https://doi.org/10.57745/VVQ2X9, 2022.

Lamprea, K. and Ruban, V.: Pollutant concentrations and fluxes in both stormwater and wastewater at the outlet of two urban watersheds in Nantes (France), Urban Water Journal, 8, 219–231, https://doi.org/10.1080/1573062X.2011.596211, 2011.

Langlois, J. L. and Mehuys, G. R.: Intra-storm study of solute chemical composition of overland flow water in two agricultural fields, J Environ Qual, 32, 2301–2310, https://doi.org/10.2134/jeq2003.2301, 2003.

Le, H. T., Pommier, T., Ribolzi, O., Soulileuth, B., Huon, S., Silvera, N., and Rochelle-Newall, E.: Overland flow during a storm event strongly affects stream water chemistry and bacterial community structure, Aquatic Sciences - Research Across Boundaries, 84, 7, https://doi.org/10.1007/s00027-021-00839-y, 2022.

Li, P. and Hur, J.: Utilization of UV-Vis spectroscopy and related data analyses for dissolved organic matter (DOM) studies: A review, Critical Reviews in Environmental Science and Technology, 47, 131–154, https://doi.org/10.1080/10643389.2017.1309186, 2017.

Lin, B., An, X., Zhao, C., Gao, Y., Liu, Y., Qiu, B., Qi, F., and Sun, D.: Analysis of urban composite non-point source pollution characteristics and its contribution to river DOM based on EEMs and FT-ICR MS, Water Research, 266, 122406, https://doi.org/10.1016/j.watres.2024.122406, 2024.

Liu, W.-R., Zeng, D., She, L., Su, W.-X., He, D.-C., Wu, G.-Y., Ma, X.-R., Jiang, S., Jiang, C.-H., and Ying, G.-G.: Comparisons of pollution characteristics, emission situations, and mass loads for heavy metals in the manures of different

livestock and poultry in China, Science of the Total Environment, 734, https://doi.org/10.1016/j.scitotenv.2020.139023, 2020.

Liu, Y., Walling, D. E., Yang, M., and Zhang, F.: Sediment source fingerprinting and the temporal variability of source contributions, Journal of Environmental Management, 338, 117835, https://doi.org/10.1016/j.jenvman.2023.117835, 2023.

Madani, E. M., Jansson, P. E., and Babelon, I.: Differences in water balance between grassland and forest watersheds using long-term data, derived using the CoupModel, Hydrology Research, 49, 72–89, https://doi.org/10.2166/nh.2017.154, 2017.

Marti, R., Ribun, S., Aubin, J.-B., Colinon, C., Petit, S., Marjolet, L., Gourmelon, M., Schmitt, L., Breil, P., Cottet, M., and Cournoyer, B.: Human-driven microbiological contamination of benthic and hyporheic sediments of an intermittent peri-urban river assessed from MST and 16S rRNA genetic structure analyses, Frontiers in Microbiology, 8, 19, https://doi.org/10.3389/fmicb.2017.00019, 2017.

Martins, J., Coquery, M., Robinet, N., Nord, G., Duwig, C., Legout, C., Morel, M. C., Spadini, L., Hachgenei, N., Némery, J., Mao, P., Margoum, C., Miege, C., Daval, A., Mathon, B., and Liger, L.: Origine et devenir des contaminants PHARMAceutiques dans les Bassins Versants agricoles. Le cas de la Claduègne (Ardèche). PHARMA-BV, , 2, 2019.

Masson, M., Grandjouan, O., Branger, F., Brosse, C., Dherret, L., Lagouy, M., Richard, L., and Coquery, M.: Analyses de paramètres majeurs et métaux dissous dans les échantillons de sources des bassins versants du Ratier et du Mercier (Lyon, France), https://doi.org/10.57745/HQPIFQ, 2025a.

Masson, M., Grandjouan, O., Branger, F., Brosse, C., Dherret, L., Lagouy, M., Richard, L., and Coquery, M.: Analyses des indicateurs optiques de la matière organique dissoute mesurés dans les échantillons de sources des bassins versants du Ratier et du Mercier (Lyon, France), https://doi.org/10.57745/IYJ2VE, 2025b.

McDonnell, J. J., Spence, C., Karran, D. J., van Meerveld, H. J. (Ilja), and Harman, C. J.: Fill-and-Spill: A Process Description of Runoff Generation at the Scale of the Beholder, Water Resources Research, 57, e2020WR027514, https://doi.org/10.1029/2020WR027514, 2021.

McElmurry, S. P., Long, D. T., and Voice, T. C.: Stormwater dissolved organic matter: Influence of land cover and environmental factors, Environmental Science and Technology, 48, 45–53, https://doi.org/10.1021/es402664t, 2014.

Mejía, A. I. and Moglen, G. E.: Impact of the spatial distribution of imperviousness on the hydrologic response of an urbanizing basin, Hydrological Processes, 24, 3359–3373, https://doi.org/10.1002/hyp.7755, 2010.

Motha, J. A., Wallbrink, P. J., Hairsine, P. B., and Grayson, R. B.: Determining the sources of suspended sediment in a forested catchment in southeastern Australia, Water Resources Research, 39, https://doi.org/10.1029/2001WR000794, 2003.

Nguyen, H., Peche, A., and Venohr, M.: Modelling Of Sewer Exfiltration To Groundwater In Urban Wastewater Systems: A Critical Review, Journal of Hydrology, 126130, https://doi.org/10.1016/j.jhydrol.2021.126130, 2021.

Omogbehin, M. H. and Oluwatimilehin, I. A.: Changes of water chemistry from rainfall to stream flow in Obagbile Catchment, Southwest Nigeria, Regional Sustainability, 3, 170–181, https://doi.org/10.1016/j.regsus.2022.07.006, 2022.

Penuelas, J., Coello, F., and Sardans, J.: A better use of fertilizers is needed for global food security and environmental sustainability, Agriculture & Food Security, 12, 5, https://doi.org/10.1186/s40066-023-00409-5, 2023.

Peuravuori, J. and Pihlaja, K.: Molecular size distribution and spectroscopic properties of aquatic humic substances, Analytica Chimica Acta, 337, 133–149, https://doi.org/10.1016/S0003-2670(96)00412-6, 1997.

Pozzi, A. C. M., Petit, S., Marjolet, L., Youenou, B., Lagouy, M., Namour, P., Schmitt, L., Navratil, O., Breil, P., Branger, F., and Cournoyer, B.: Ecological assessment of combined sewer overflow management practices through the analysis of benthic and hyporheic sediment bacterial assemblages from an intermittent stream, Science of The Total Environment, 907, 167854, https://doi.org/10.1016/j.scitotenv.2023.167854, 2024.

Rai, S. P., Singh, D., Jacob, N., Rawat, Y. S., Arora, M., and BhishmKumar: Identifying contribution of snowmelt and glacier melt to the Bhagirathi River (Upper Ganga) near snout of the Gangotri Glacier using environmental isotopes, CATENA, 173, 339–351, https://doi.org/10.1016/j.catena.2018.10.031, 2019.

Ramon, R.: Quantifying sediment source contributions in contrasted agricultural catchments (Uruguay River, Southern Brazil), Theses, Thèse de doctorat, Université Paris-Saclay ; Universidade Federal do Rio Grande do Sul (Porto Alegre, Brésil), 2021.

Robinson, M. and Dupeyrat, A.: Effects of commercial timber harvesting on streamflow regimes in the Plynlimon catchments, mid-Wales, Hydrological Processes, 19, 1213–1226, https://doi.org/10.1002/hyp.5561, 2005.

Sandin, M., Piikki, K., Jarvis, N., Larsbo, M., Bishop, K., and Kreuger, J.: Spatial and temporal patterns of pesticide concentrations in streamflow, drainage and runoff in a small Swedish agricultural catchment, Sci Total Environ, 610–611, 623–634, https://doi.org/10.1016/j.scitotenv.2017.08.068, 2018.

Sanisaca, L. E. G., Gellis, A. C., and Lorenz, D. L.: Determining the sources of fine-grained sediment using the Sediment Source Assessment Tool (Sed_SAT), Open-File Report, Reston, VA, https://doi.org/10.3133/ofr20171062, 2017.

Sarrazin, B.: MNT et observations multi-locales du réseau de drainage d'un petit bassin versant rural dans une perspective d'aide à la modélisation spatialisée, Theses, Thèse de doctorat, Université Grenoble Alpes, 2012.

Shi, M.-M., Wang, X.-M., Chen, Q., Han, B.-H., Zhou, B.-R., Xiao, J.-S., and Xiao, H.-B.: Responses of soil moisture to precipitation and infiltration in dry and wet alpine grassland ecosystems, Acta Prataculturae Sinica, 30, 49–58, https://doi.org/10.11686/cyxb2020436, 2021.

Simpson, I. M., Winston, R. J., and Dorsey, J. D.: Monitoring the effects of urban and forested land uses on runoff quality: Implications for improved stormwater management, Science of The Total Environment, 862, 160827, https://doi.org/10.1016/j.scitotenv.2022.160827, 2023.

Singh, S. K. and Stenger, R.: Indirect methods to elucidate water flows and contaminant transfer pathways through meso-scale catchments – A review, Environmental Processes, 5, 683–706, https://doi.org/10.1007/s40710-018-0331-6, 2018.

Spence, C. and Woo, M.: Hydrology of subarctic Canadian shield: soil-filled valleys, Journal of Hydrology, 279, 151–166, https://doi.org/10.1016/S0022-1694(03)00175-6, 2003.

Stock, B. C., Jackson, A. L., Ward, E. J., Parnell, A. C., Phillips, D. L., and Semmens, B. X.: Analyzing mixing systems using a new generation of Bayesian tracer mixing models, PeerJ, 6, 2018.

Sun, Z.-X., Cui, J.-F., Cheng, J.-H., and Tang, X.-Y.: A novel tool for tracing water sources of streamflow in a mixed land-use catchment, Science of The Total Environment, 912, 168800, https://doi.org/10.1016/j.scitotenv.2023.168800, 2024.

Tardy, Y., Bustillo, V., and Boeglin, J.-L.: Geochemistry applied to the watershed survey: hydrograph separation, erosion and soil dynamics. A case study: the basin of the Niger River, Africa, Applied Geochemistry, 19, 469–518, https://doi.org/10.1016/j.apgeochem.2003.07.003, 2004.

Thorndike, R. L.: Who belongs in the family?, Psychometrika, 18, 267–276, https://doi.org/10.1007/BF02289263, 1953.

Tiecher, T., Caner, L., Minella, J. P. G., and dos Santos, D. R.: Combining visible-based-color parameters and geochemical tracers to improve sediment source discrimination and apportionment, Science of The Total Environment, 527–528, 135–149, https://doi.org/10.1016/j.scitotenv.2015.04.103, 2015.

Tran, N. H., Reinhard, M., Khan, E., Chen, H., Nguyen, V. T., Li, Y., Goh, S. G., Nguyen, Q. B., Saeidi, N., and Gin, K. Y.-H.: Emerging contaminants in wastewater, stormwater runoff, and surface water: Application as chemical markers for diffuse sources, Science of The Total Environment, 676, 252–267, https://doi.org/10.1016/j.scitotenv.2019.04.160, 2019.

Tromp-van Meerveld, H. J. and McDonnell, J.: Threshold relations in subsurface stormflow: 2. The fill and spill hypothesis, Water Resources Research, 42, https://doi.org/10.1029/2004WR003800, 2006.

Uber, M., Legout, C., Nord, G., Crouzet, C., Demory, F., and Poulenard, J.: Comparing alternative tracing measurements and mixing models to fingerprint suspended sediment sources in a mesoscale Mediterranean catchment, Journal of Soils and Sediments, 19, 3255–3273, https://doi.org/10.1007/s11368-019-02270-1, 2019.

Vale, S., Swales, A., Smith, H. G., Olsen, G., and Woodward, B.: Impacts of tracer type, tracer selection, and source dominance on source apportionment with sediment fingerprinting, Science of The Total Environment, 831, 154832, https://doi.org/10.1016/j.scitotenv.2022.154832, 2022.

Verseveld, W. J. van, McDonnell, J. J., and Lajtha, K.: A mechanistic assessment of nutrient flushing at the catchment scale, Journal of Hydrology, 358, 268–287, https://doi.org/10.1016/j.jhydrol.2008.06.009, 2008.

Vian, J.-F.: Agriculture biologique et qualité de l'eau. Etat des lieux des forces et faiblesses des systèmes de production conduits en AB, ISARA Lyon, 2019.

Walsh, C. J., Roy, A. H., Feminella, J. W., Cottingham, P. D., Groffman, P. M., and Morgan, R. P.: The urban stream syndrome: current knowledge and the search for a cure, Journal of the North American Benthological Society, 24, 706–723, https://doi.org/10.1899/04-028.1, 2005.

Wang, F., Liu, L., Xu, W., Li, Y., Ruan, Q., and Cao, W.: Multiple stable isotopic approaches for tracing nitrate contamination sources: Implications for nitrogen management in complex watersheds, Ecotoxicology and Environmental Safety, 269, 115822, https://doi.org/10.1016/j.ecoenv.2023.115822, 2024.

Wang, Y.-H., Zhang, P., He, C., Yu, J.-C., Shi, Q., Dahlgren, R. A., Spencer, R. G. M., Yang, Z.-B., and Wang, J.-J.: Molecular signatures of soil-derived dissolved organic matter constrained by mineral weathering, Fundamental Research, 3, 377–383, https://doi.org/10.1016/j.fmre.2022.01.032, 2023.

Wellington, B. I. and Driscoll, C. T.: The episodic acidification of a stream with elevated concentrations of dissolved organic carbon, Hydrological Processes, 18, 2663–2680, https://doi.org/10.1002/hyp.5574, 2004.

White, A. F., Bullen, T. D., Vivit, D. V., Schulz, M. S., and Clow, D. W.: The role of disseminated calcite in the chemical weathering of granitoid rocks, Geochimica et Cosmochimica Acta, 63, 1939–1953, https://doi.org/10.1016/S0016-7037(99)00082-4, 1999.

Wilkinson, S. N., Hancock, G. J., Bartley, R., Hawdon, A. A., and Keen, R. J.: Using sediment tracing to assess processes and spatial patterns of erosion in grazed rangelands, Burdekin River basin, Australia, Agriculture, Ecosystems and Environment, 180, 90–102, https://doi.org/10.1016/j.agee.2012.02.002, 2013.

Yokel, J. and Delistraty, D. A.: Arsenic, lead, and other trace elements in soils contaminated with pesticide residues at the Hanford site (USA), Environmental toxicology, 18, 104–114, https://doi.org/10.1002/tox.10106, 2003.